Appendix I
Sediment Transport Modelling Technical Report

Australian Government

Australian Institute of Marine Science

Modelling the sediment plume associated with dredging for the Darwin Ship Lift

Carlos Simão and Hemerson Tonin

Report prepared for AECOM

AIMS: Australia's tropical marine research agency.
www.aims.gov.au

Australian Institute of Marine Science

PMB No 3
Townsville MC Qld 4810

PO Box 41775
Casuarina NT 0811

Indian Ocean Marine Research Centre
University of Western Australia, M096
Crawley WA 6009

This report should be cited as:
Simão, C. and Tonin, H. (2020). Modelling the sediment plume associated with dredging for the Darwin Ship Lift. Prepared for AECOM. Australian Institute of Marine Science, Darwin. pp 45, including appendices

DISCLAIMER

While reasonable efforts have been made to ensure that the contents of this document are factually correct, AIMS does not make any representation or give any warranty regarding the accuracy, completeness, currency or suitability for any particular purpose of the information or statements contained in this document. To the extent permitted by law AIMS shall not be liable for any loss, damage, cost or expense that may be occasioned directly or indirectly through the use of or reliance on the contents of this document.

Project Leader shall ensure that documents have been fully checked and approved prior to submittal to client

Revision History:		*Name*	*Date*	*Comments*
1	Prepared by:	Carlos Eduardo Simao Hemerson Tonin	20/09/2020	
	Reviewed by:	Claire Streten	21/09/2020	Minor changes
	Approved by:	Richard Brinkman	20/10/2020	Approved for submission to AECOM
	Reviewed by:	Peter Young - AECOM	23/11/2020	Minor revisions
	Revised by:	Carlos Eduardo Simao and Hemerson Tonin	25/11/2020	

Cover photo:
RV Solander in Western Australia. Image: N. Thake

CONTENTS

TABLE OF FIGURES

LIST OF TABLES

1. BACKGROUND

AECOM has approached AIMS to implement a numerical sediment model in the Darwin Harbour to predict the extent of the sediment plume and deposition resulting from Stage 1 dredging activities for the construction of the Darwin Ship Lift.

2. APPROACH

2.1. Hydrodynamic model grid

The model utilized in this study is the Delft3D suite and it is presented in Appendix A: Delft3D – a brief model description.

The grid of AIMS's existing Darwin Harbour model was updated to include a high-resolution grid for the dredge footprint of the Darwin Ship Lift project and the adjacent marine environment. The grid has a 30m x 30m horizontal resolution for the dredging area, and 60m in the adjacent areas (Figure 1). The bathymetry used in the model is from Darwin Harbour Marine Survey (https://ecat.ga.gov.au/geonetwork/srv/eng/catalog.search#/metadata/100093).

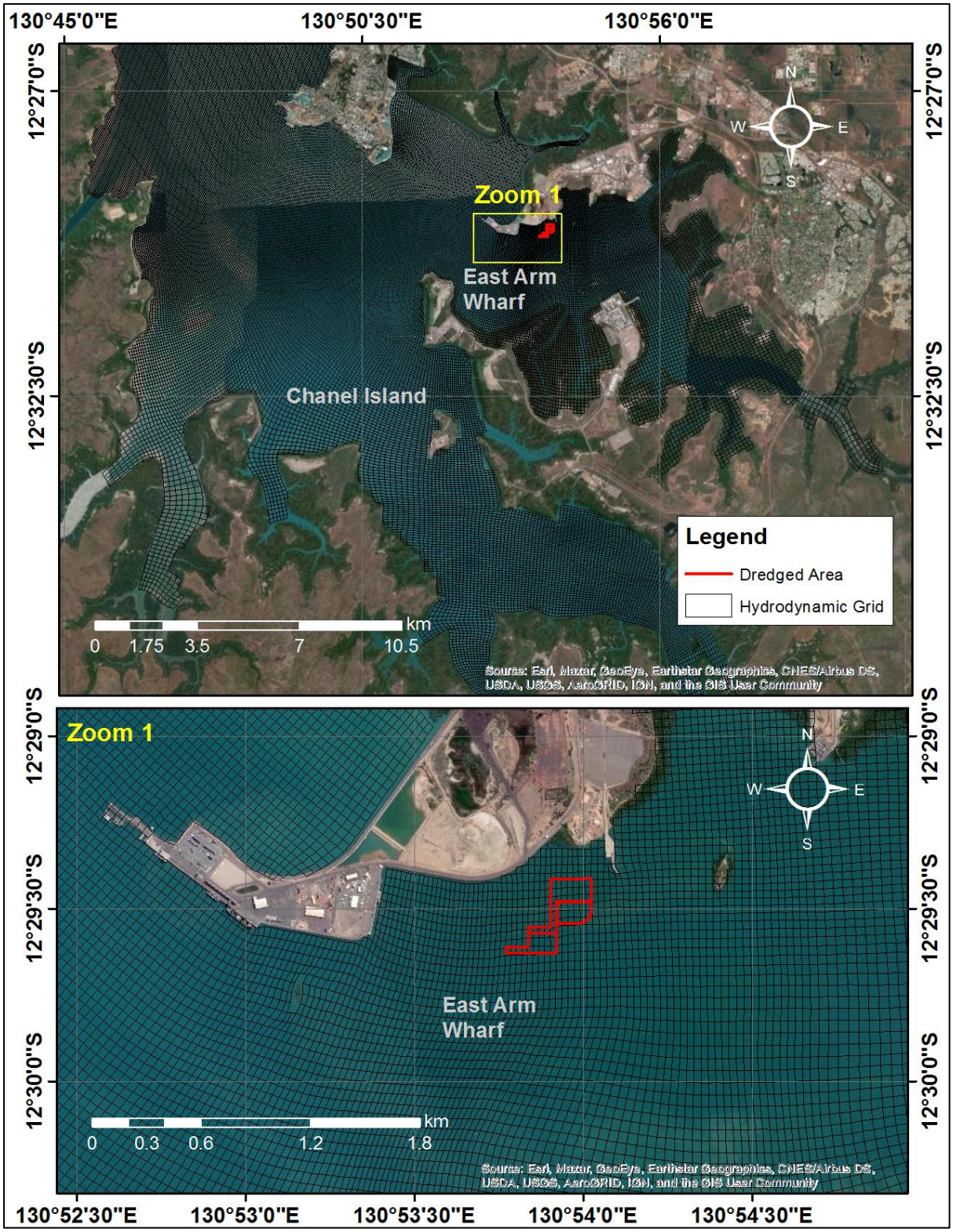

Figure 1: Hydrodynamic model grid in the regions of interest. Upper panel, the numerical grid implemented in the Darwin Port and, in the lower panel, the area to be dredged (boundaries as red lines).

2.2. Data sources and synthesis for model input

Wind and Tide data

The wind data used in this study was collected at the Darwin National Reference Station (NRS) mooring located at Latitude: -12.3382, Longitude: 130.6952. Wind data for the entire years of 2017 and 2018 were used (Figure 2).

The hydrodynamic circulation in Darwin Harbour is predominantly driven by tides. The tidal data used to force the model was from the Nightcliff station (see Figure 2), provided by JTides (https://arachnoid.com/JTides/index.html). Tidal data from a tide gauge deployed nearby the target location was also used to validate the model (Figure 2).

Figure 2: Geographical location of data sources used in the meteo-oceanographic characterization of the region and in the current modelling study.

2.3. Assessing model skill to replicate hydrodynamics

To assess the skill of the model, measured sea surface elevations were compared with the predicted tide results from the hydrodynamic model for the period of 12-Dec-2017 to 30-Dec-2017. The comparison between the time series of simulated sea surface elevation (as output of the numerical model) and the observed sea surface elevation were assessed using the methodology described in Wilmott (1981). The model skill proposed by Wilmott is commonly used in the scientific literature for the comparison of two time series, where *X* is the variable being compared with a time mean $\overline{X}$ (see Equation 1). Perfect agreement between the model results and the observations will produce a skill of one and complete disagreement will produce a skill of zero.

$$Skill = 1 - \frac{\sum|X_{model} - X_{obs}|^2}{\sum\left(|X_{model} - \overline{X_{obs}}| + |X_{obs} - \overline{X_{obs}}|\right)^2} \qquad \text{Equation 1}$$

2.4. Modelling background suspended sediment concentrations

Background suspended sediment concentrations for the area of interest were established by running a numerical simulation in the absence of dredging thus suspended sediment concentrations in the water column will be the result of resuspension driven by the hydrodynamics of the region. The numerical simulation run without dredging is referred to as Scenario 01 throughout this report.

The seabed sediment composition used in Scenario 01 was based on three different sources (Figure 3). The first data source used was a study that extensively mapped and classified the Darwin Harbour seabed sediments (Siwabessy, et al., 2015). The second source was the particle size distribution (PSD) provided by AECOM (Appendix B). For the AECOM data an averaged particle size distribution value was calculated for each data point and used in the modelling grid composition. The last source of data used was a study of sediment transport and bed material to support the Darwin Harbour sediment transport model (Patterson, R.G. and Williams, D.K. 2014). The data from the three studies was integrated into the sediment map and linearly distributed into the grid model as the initial condition for Scenario 01 (Figure 4).

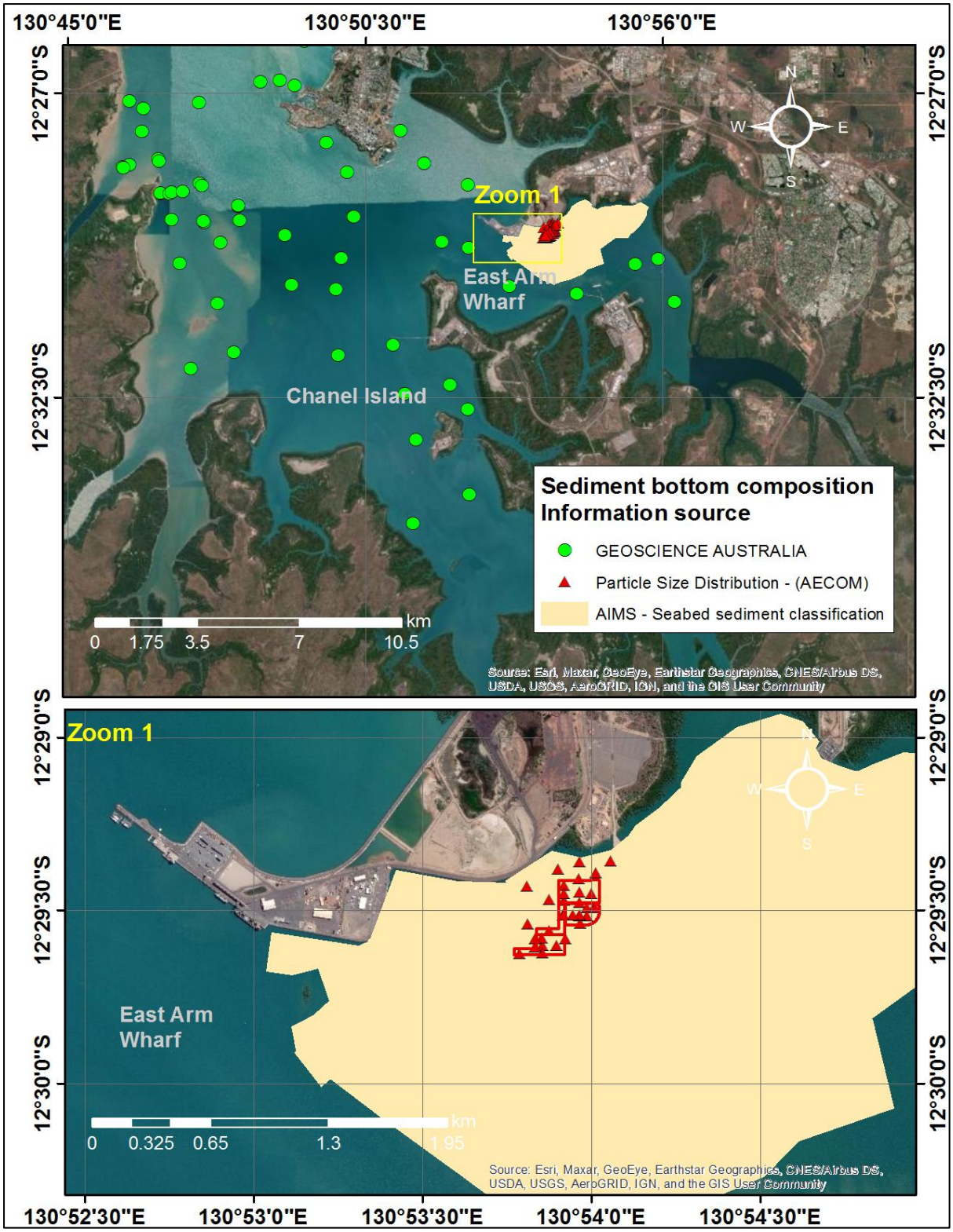

Figure 3: Spatial distribution of sediment composition data.

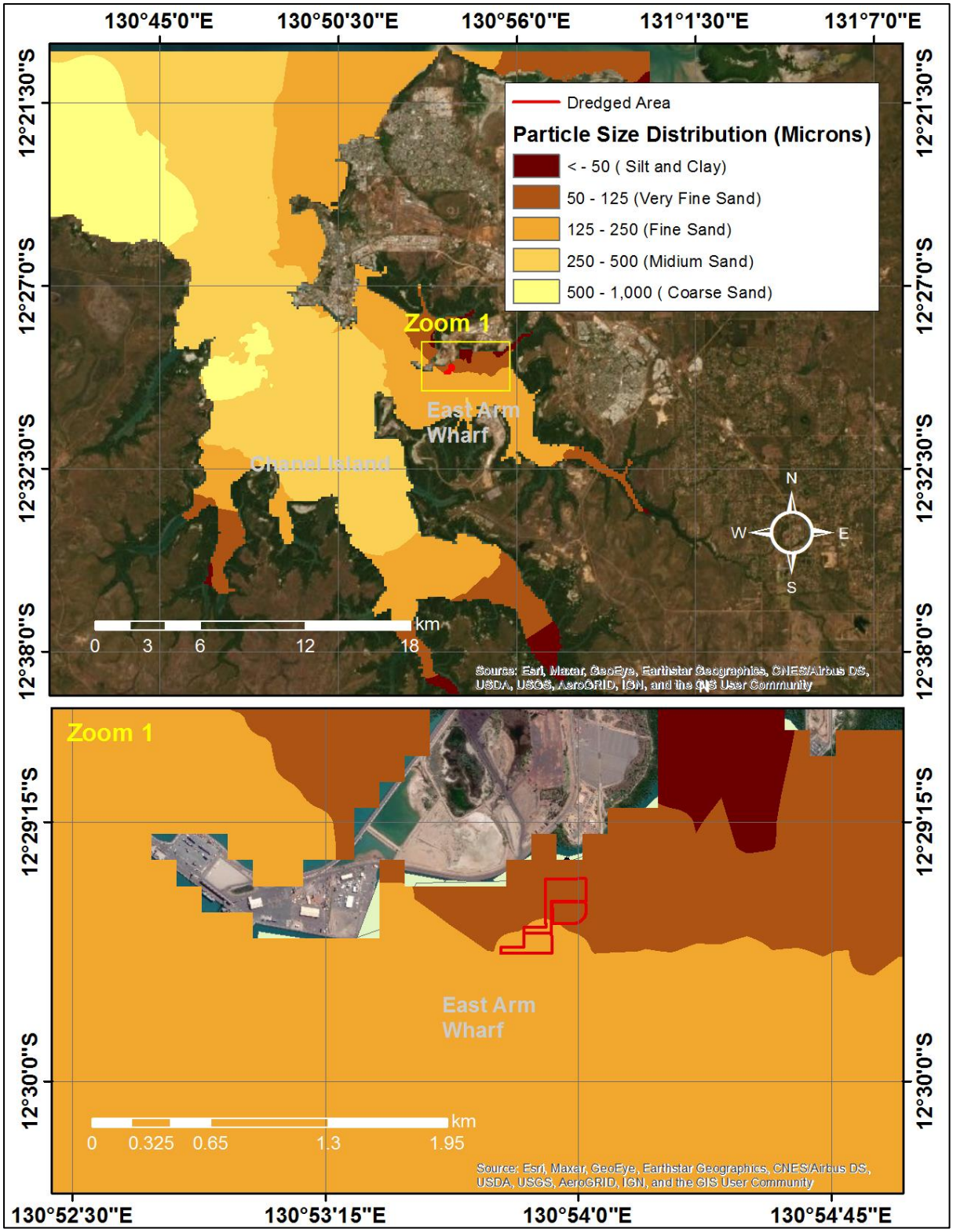

Figure 4: Seabed particle size distribution used for Scenario 01 (background)modelling.

The sediment at seabed surface was combined in 4 classes (clay, silty, sand, gravel) according to its granulometry (Table 1). Settling velocity for each class of sediment in the dredging model were assigned based on values commonly found in the literature (for more details see Makarynskyy et al 2017) and are presented in (Table 1).

Critical erosion stress is usually classified by field experiment, however in situations where field data is not available a value from the scientific literature can be applied. According to Li (2016) the Critical Shear Stress value of 1.0 Nm^{-2} can be used in tidal flats and mangrove areas. The critical erosion stresses applied in the modelling scenarios are presented in Table 2.

Table 1: Typical settling velocity (in mm/s) by class of sediment

Sediment type	*w^* (mm/s)*
Gravel	242.0
Sand	38.885
Silt	0.182
Clay	0.0022

w^*, settling velocity (mm/s)

Table 2: Resuspension/critical erosion threshold applied for the different sediment classes

Sediment type	*Critical Shear Stress (Nm^2)*
Gravel	2.7
Sand	0.1
Silt	1
Clay	1

The numerical simulation of background SSC was run for the time period of Nov-2017 to Jun-2018, using the Nightcliff tidal harmonics and hourly winds from the NRS Darwin buoy as forcing. The background SSC concentrations were compared to those reached during dredging operations.

2.5. Modelling SSC, sediment deposition and removal during and post dredging

2.5.1. Dredging location and volume

The overall region to be dredged comprises a location in the East Arm of the Darwin Harbour (Figure 5). The dredging operation intends to remove a total of 324,800m^3 of sediment (sum of all regions to be dredged). Sediment composition used in the modelling was based on the PSD data which was made available by AECOM (Appendix B: particle size distribution (PSD)).

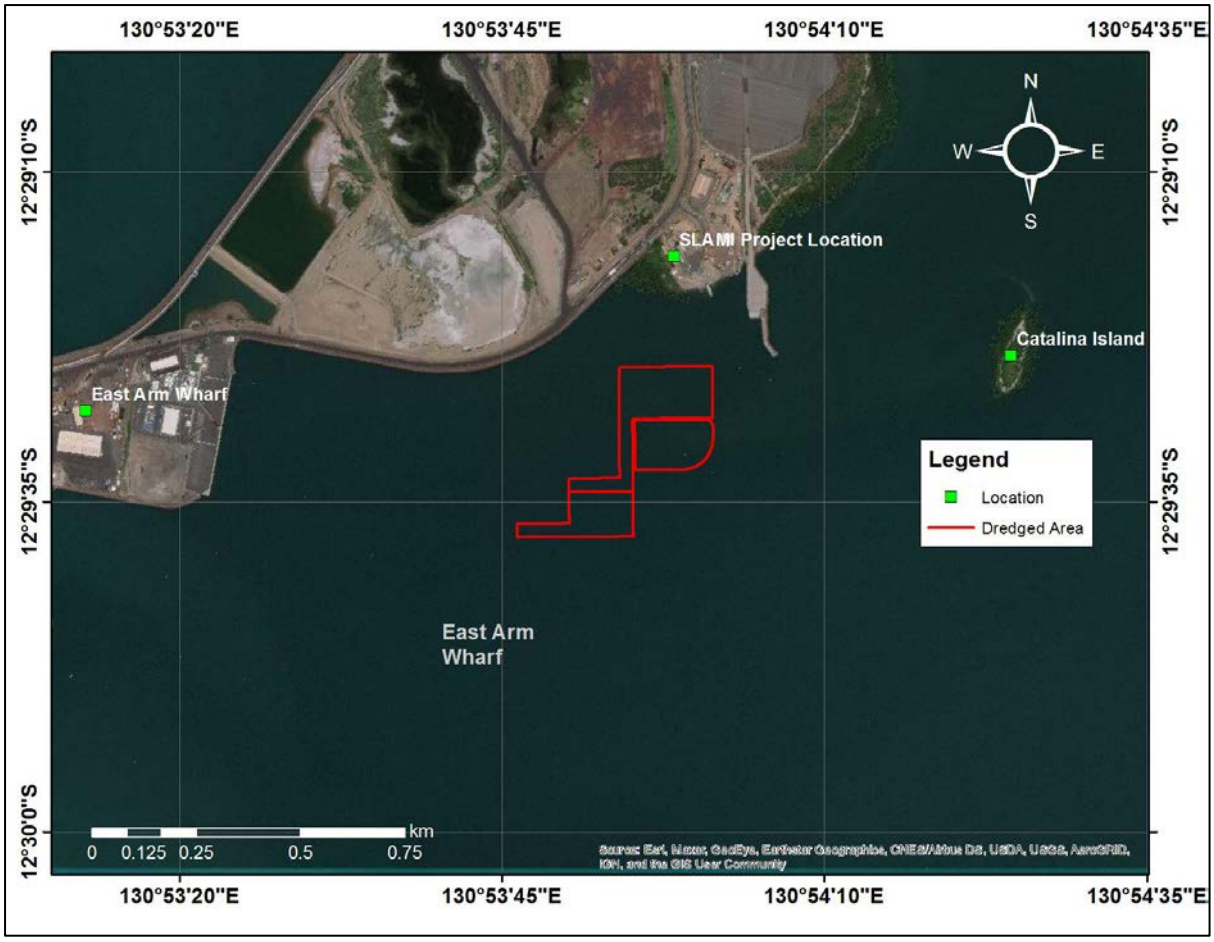

Figure 5: Boundaries of the areas to be dredged are shown as red lines (boundaries).

2.5.2. Dredging equipment methodology

The transport and fate of sediments released during dredging operations was modelled based on the use of a small Cutter Suction Dredger (CSD). Using a CSD the dredging operations should take 23.2 weeks (information made available by AECOM in a document: SLAMI Early Works Dredging Sediment Transport Modelling Parameter).

The designed hourly production during a day of dredging operation is presented in Table 3. The dredging operation was simulated to follow the continuous production cycle (Table 3) until the entire planned dredged volume was completed.

Table 3: Designed hourly production (in m^3/hr) during a 24 day of dredging operation

Time (h)	Production (m^3/hr)	Dredge head loss (m^3/hr)
1	150	7.5
2	150	7.5
3	75	3.75
4	50	2.5
5	0	0
6	0	0
7	0	0
8	50	2.5
9	75	3.75
10	150	7.5
11	150	7.5
12	150	7.5
13	150	7.5
14	150	7.5
15	150	7.5
16	75	3.75
17	50	2.5
18	0	0
19	0	0
20	0	0
21	50	2.5
22	75	3.75
23	150	7.5
24	150	7.5

2.5.3. Dredge modelling methodology

The dredging operation was simulated in the model by making the mass of sediment available at the grid cell according to the production rate of the dredging operation and the volume to be removed, at specific points of the model grid (Table 3).

Another source of sediment is the loss of sediment at the dredge head. During the dredging operation, since the seabed is disturbed by dredging, a fraction of the sediment is lost as it is not captured as dredged material. This fraction is named as dredge head loss and it was set as 5% of the production rate as established by AECOM in the document SLAMI Early Works Dredging Sediment Transport Modelling Parameter (Table 3). The time interval for the dredge head loss was implemented based on the dredging cycles (Table 3). The sediment to be dredged and the dredge head loss were implemented as sediment sources in the numerical model grid, simulating a CSD operation. Notice, as there is no overflow in the proposed dredging process only dredge head loss was considered.

The sediment composition applied to the sediment source was based on the median particle size distribution for clay, silt, sand and gravel calculated from the data provided by AECOM (Appendix B).

Sediments of two different compositions were modelled as part of the study – these are referred to as Scenario 02 and 03 (Table 4). Scenario 03 was similar to Scenario 02 with a 50% increase in fine particles fractions (clay and silt) only, based on the PSD. In that scenario, the percentage distribution of sediments was adjusted to increase fines and preserve the total mass by reducing larger particle sizes. Scenario 03 was run to understand how an increase in fine particles in the dredged material would influence the extent of the sediment plume associated with dredge operations.

Table 4: Mean particle size percentual distribution based on PSD

Scenario name	Clay (%)	Silt (%)	Sand (%)	Gravel (%)
Scenario 02	16.7	17.0	38.8	27.5
Scenario 03	25.0	25.5	30.0	19.5

The period simulated for the model was 163 days, plus 30 days after the dredging had ceased. The latter period was considered to assess the behaviour of sediment in the region after the dredging has ceased. The numerical simulation of the dredging operation was carried out from Nov-2017 up to Jun-2018, using the Nightcliff tidal harmonics and hourly winds from the NRS Darwin buoy as forcing (see Figure 2 for their location).

3. . RESULTS AND DISCUSSION

3.1. Assessment of hydrodynamic model's ability to represent local environment

For the assessment of model performance, the hydrodynamic model was run for the month of December of 2017. The predicted sea surface elevations were validated against the sea surface elevation measured at one location (see Figure 2).

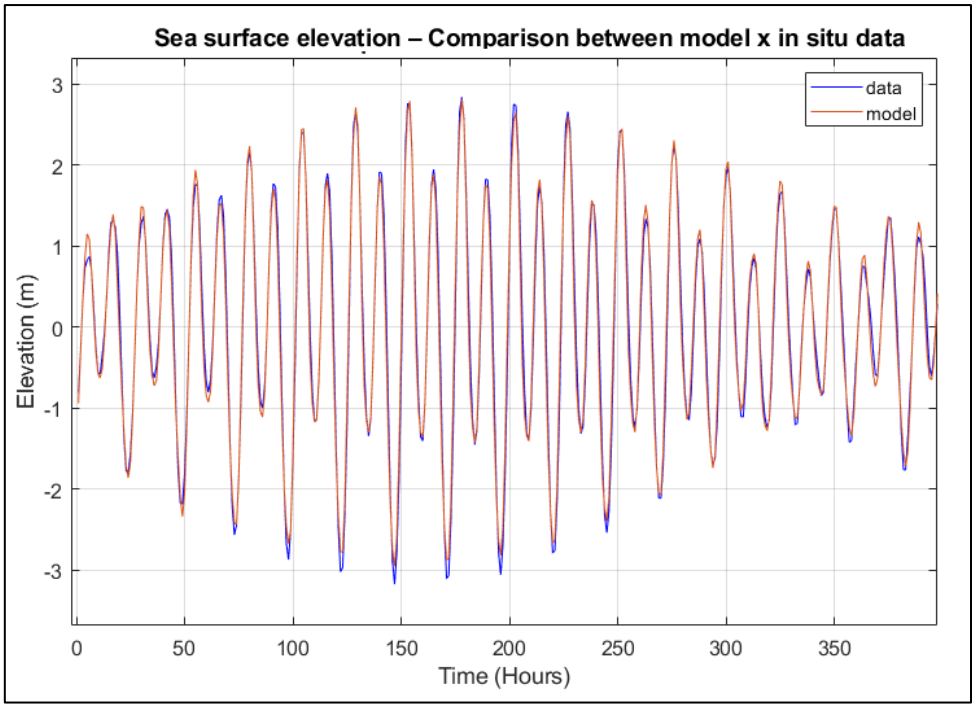

Figure 6: Comparison between the time series of sea surface elevation at East Arm as output of numerical model (red) and as from *in situ* data (blue).

The Wilmot skill score based on modelled and measured sea surface elevation at the tide gauge (Figure 2) was 0.98. Perfect agreement between the model results and the observations will produce a skill of one and complete disagreement will produce a skill of zero, thus the hydrodynamic model demonstrates a high level of accuracy in simulating local conditions.

3.2. Numerically modelled suspended sediment concentrations

3.2.1. Predicted background suspended sediment due to natural processes

Numerical modelling of the background sediment movement in the region of interest (i.e. without dredging) showed that for 90% of the modelled period (Nov-2017 to Jun-2018) SSC in the vicinity of the proposed Ship Lift did not exceed 100 mg/L as a result of natural sediment resuspension (Figure 7). Under the background modelling scenario, 99% of the time the SSC in the area between East Arm boat ramp and East Arm wharf were < 100mg/L (Figure 8). The modelling result for the Scenario 01 agrees with the study carried out by URS (2011). In that study, percentiles related to the levels of SSC around the East Arm during wet season were 99% of the time below 36.5 mg/L and 95% of the time below 26.4 mg/L (disregarding nearshore areas). Furthermore, according to Li (2016) maximum SSC values over 100 mg/L were observed at point EA1 which is located at the East Arm. The URS (2011) also registered a maximum value of 83 mg/L nearby South Shell Island. Results of numerical modeling carried out by Andutta et al, (2014) showed, during spring tides, a maximum concentration above 500 mg/L at the entrance to the Port of Darwin and around 120 mg/L in the vicinity of the East Arm. . Brinkman and Logan (2019) states that the sediment at the Darwin Harbor region is easily suspended and remains in suspension, due to large tidal currents. Results from those authors cited have presented the same SSC magnitude and behaviour as predicted by Scenario 01.

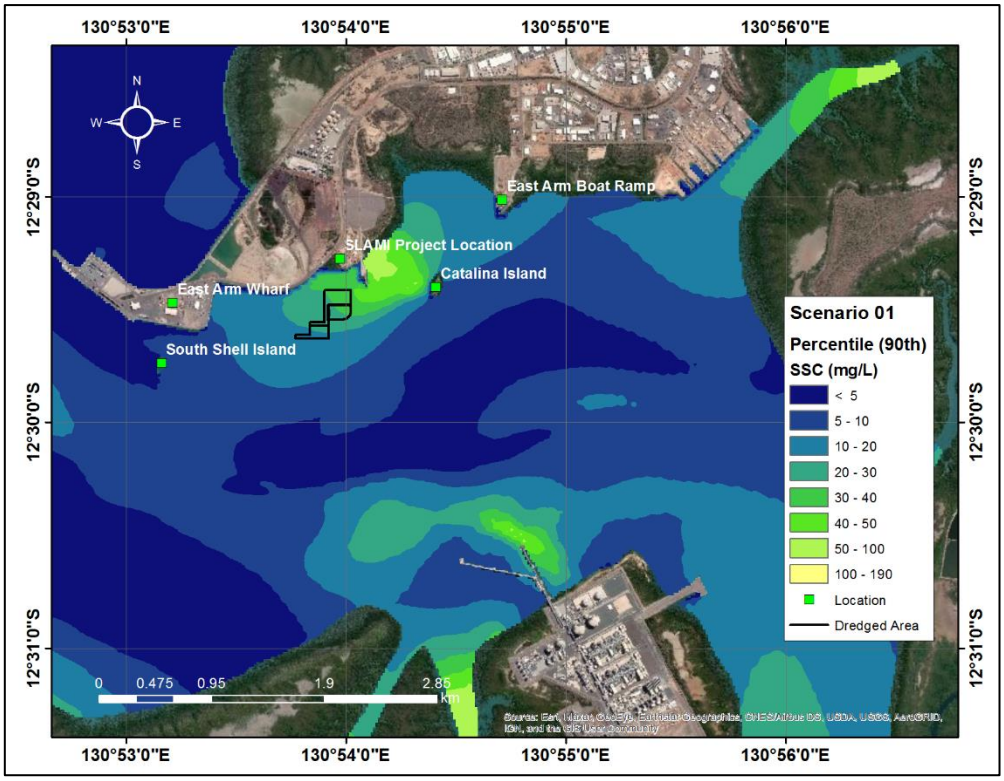

Figure 7: Spatial limits of the area subjected to 90th percentile of suspended sediment concentrations in the water column based on numerical modelling of Scenario 01 (background).

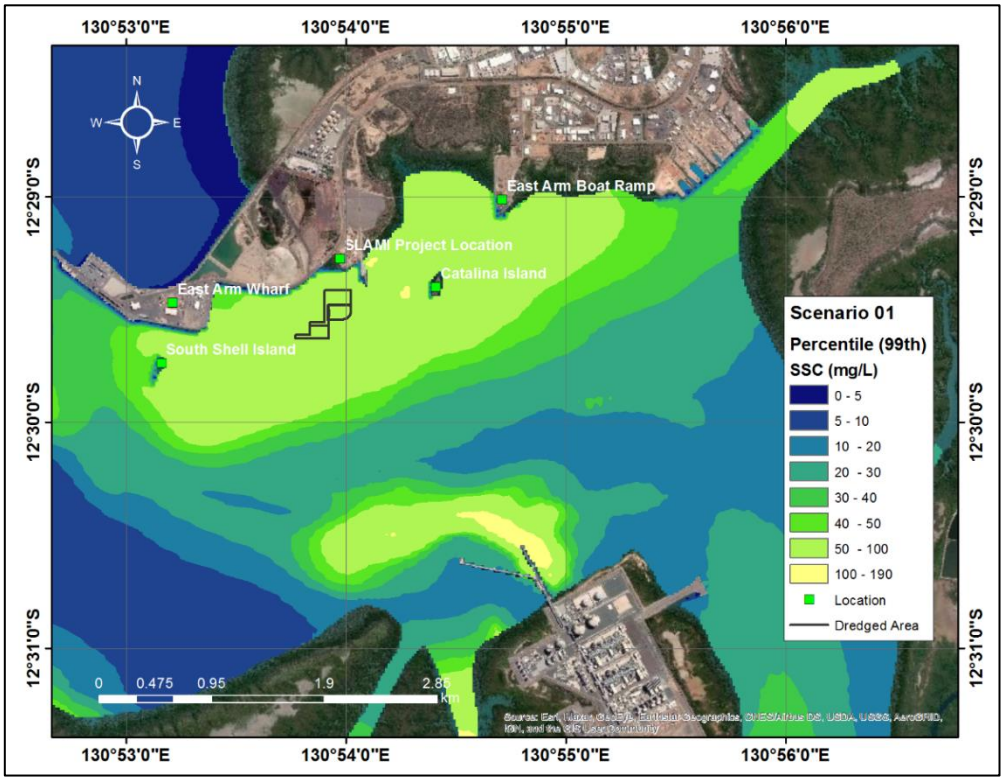

Figure 8: Spatial limits of the area subjected to 99th percentile suspended sediment concentration in the water column based on numerical modelling of Scenario 01 (background).

To understand the temporal behaviour of background SSC time series plots were generated for 8 locations near the proposed Ship Lift (Figure 9). The time series graph demonstrate background SSC have a tidal pattern and areas in the harbour are exposed to elevated concentrations during the spring tides (Figure 10 and 11). Points located in the deep water, such as P2 and P3, presented 22 mg/L as maximum SSC. The point P1 has the lowest maximum SSC, about 12 mg/L (Figure 10). The highest SSC observed was about 70 mg/L at P7 and P8, both located in a relatively shallow water and susceptible to the sediment resuspension (Figure 11).

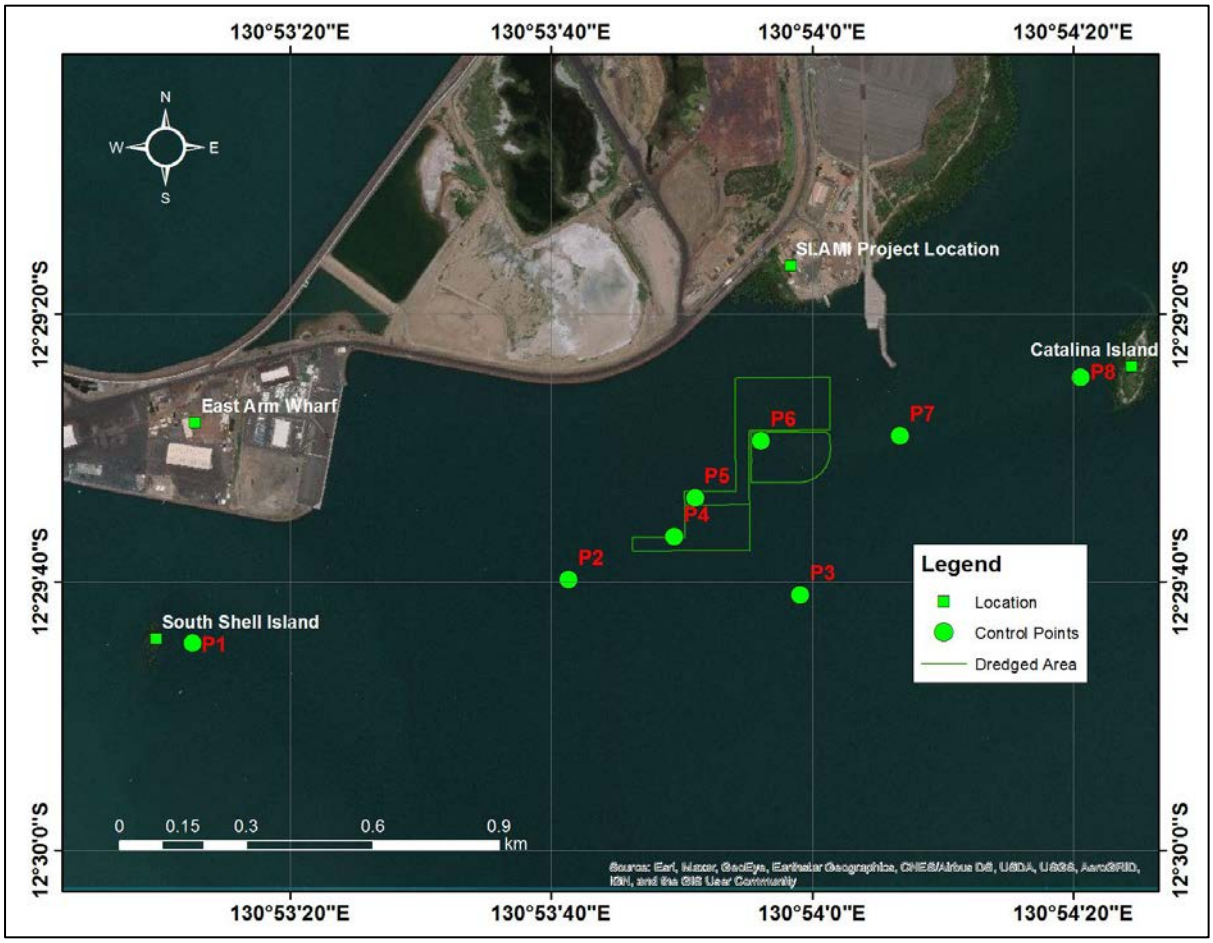

Figure 9: Set of observations points to assess temporal behaviour of SSC in numerical modelling.

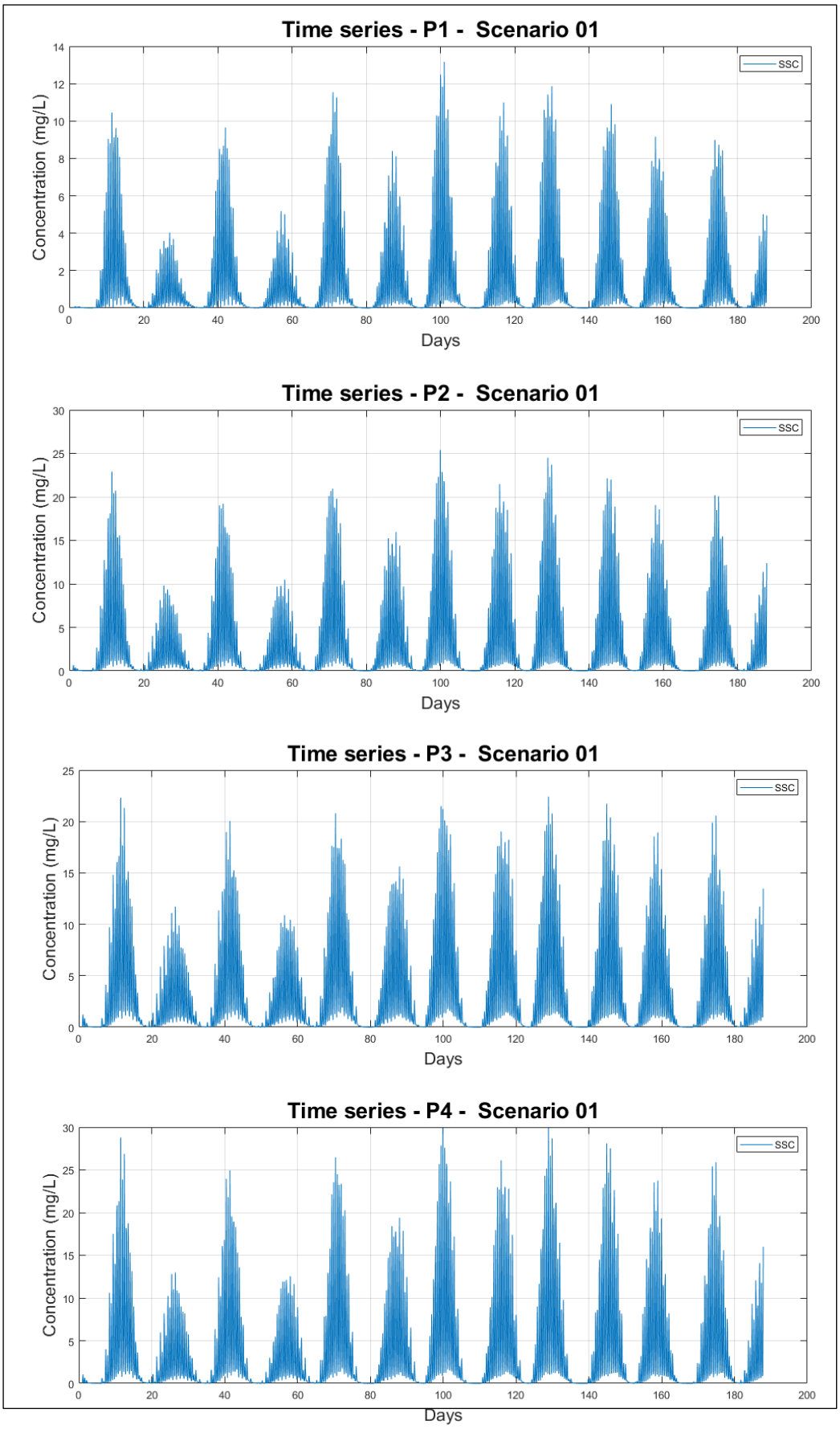

Figure 10: Time series of the maximum SSC (mg/L) at P1, P2, P3 and P4, in the water column as result of Scenario 01 (background) numerical modelling.

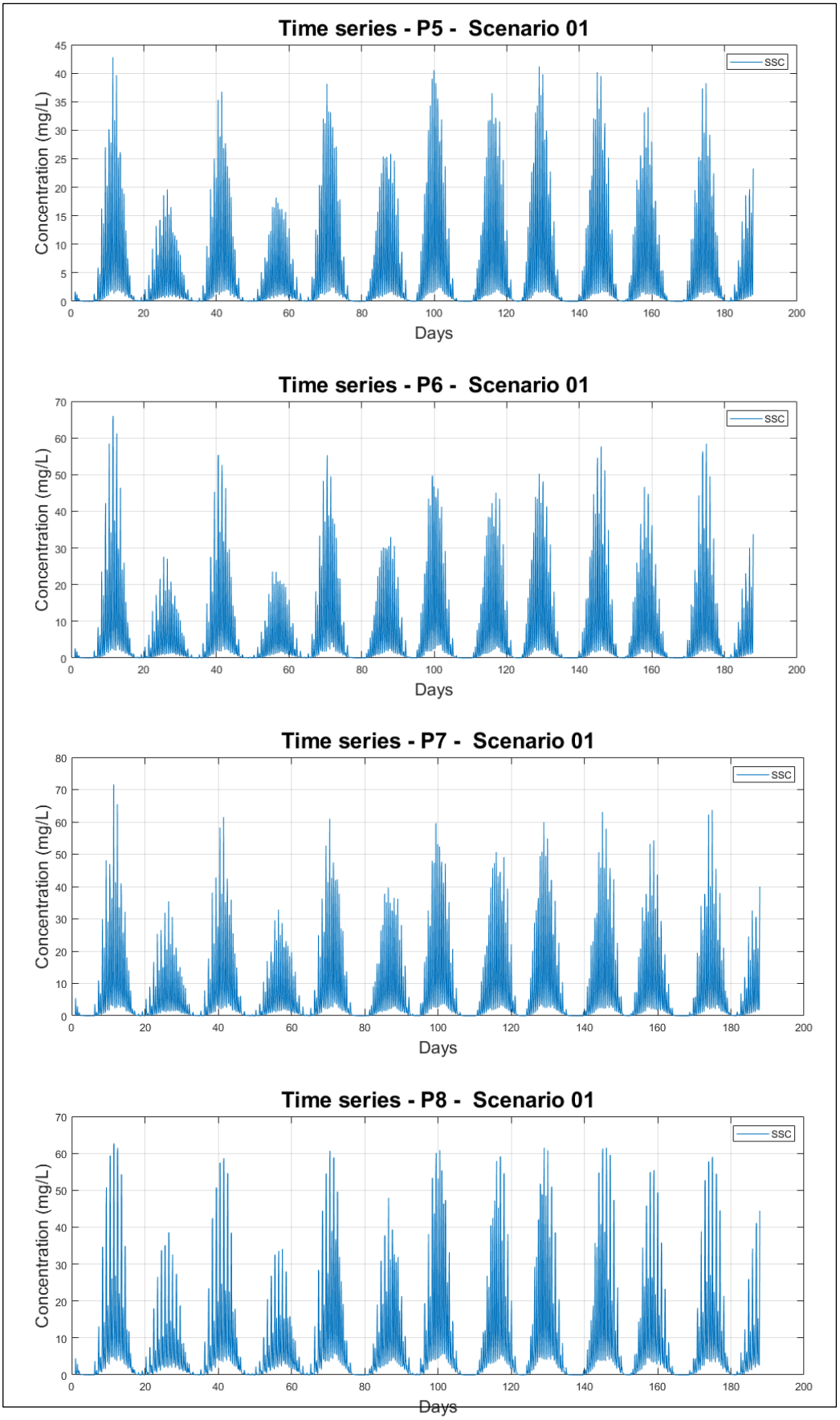

Figure 11: Time series of the maximum SSC (mg/L) at P5, P6, P7 and P8, in the water column as result of Scenario 01 (background) numerical modelling.

3.2.1. Spatial pattern of suspended sediment concentrations during dredging operations

Background SSC were not included in the modelling of the dredging operations therefore SSC during dredging is referring to the concentration above background levels.

Under Scenario 02 sediment modelling (34% of sediment < 20 µm), the simulated SSC for the Scenario 02 did not exceed 6 mg/L for 90% of the time while for Scenario 03 where the dredged sediment had a greater percentage of fine particles (50% of sediment < 20 µm) the 90th percentile SSC was 8 mg/L (Figures 12 and 13) In addition the extent of the area experiencing SSC > 5mg/L was considerably larger for Scenario 03 compared to Scenario 02 (Figures 12 and 13). Based on the 95th percentiles the SSC concentrations did not exceed 7.5 mg/L for Scenario 02 while for Scenario 03 concentrations fell below 11.5 mg/L (Figures 14 and 15). Thus, under Scenario 03, the 10 mg/L threshold is exceeded when referencing the 95th percentile, however, the threshold is only exceeded in close proximity to the dredge operation (Figures 14 and 15). The 10 mg/L threshold is exceeded close to the dredge operations under Scenario 02 when considering the 99th percentile (Figure 16). Under Scenario 02 the zonal length subject to SSC above 2 mg/L, based on 99th percentile, is about 3.5 km (west to east), limited in the west by the Marine Supply Base and extending east to the East Arm Boat Ramp (Figure 16). For Scenario 03, SSC concentrations did not exceed 18.5 mg/L based on the 99th percentile (Figure 17). Under the 95th and 99th percentiles for Scenario 03, SSC will reach levels 5 mg/L above background at South Shell Island (Figures 15 and 17).

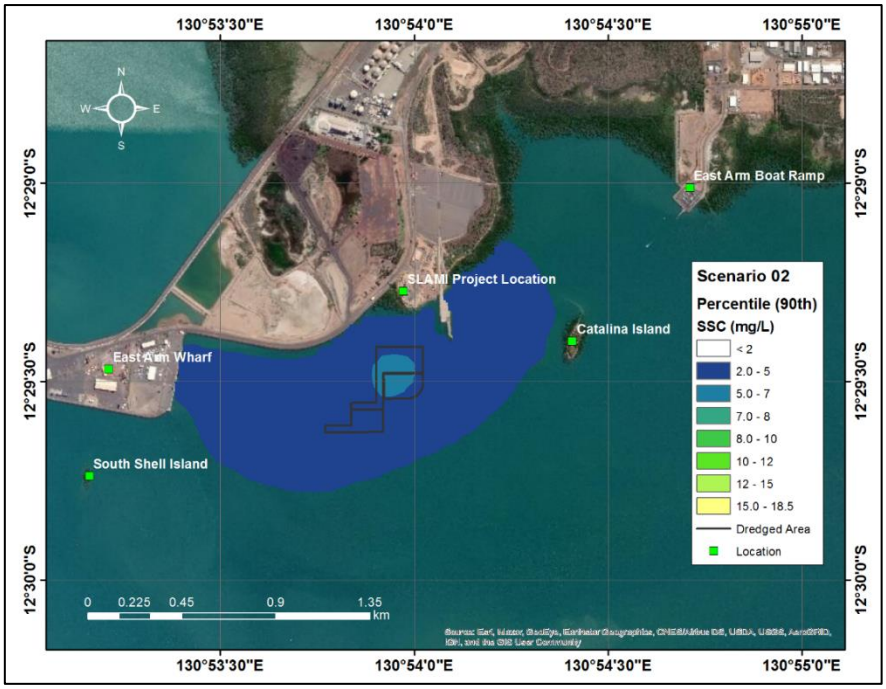

Figure 12: Spatial limits of the area subjected to 90th percentile of SSC in the water column (above background level) based on Scenario 02 where the dredged sediment composition is 30% of sediment particles < 20µm.

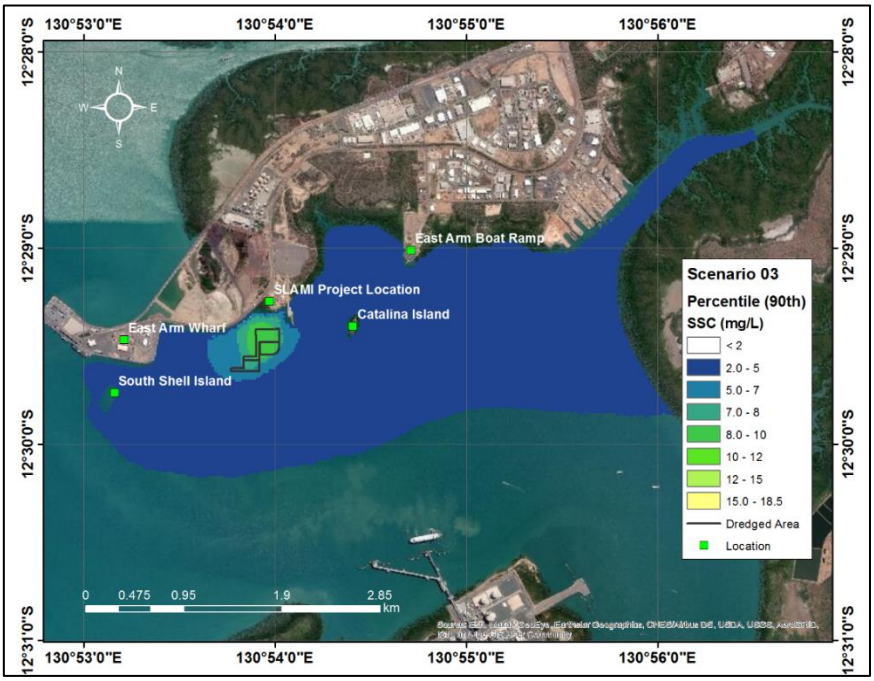

Figure 13: Spatial limits of the area subjected to 90th percentile of SSC in the water column (above background level) based on Scenario 03 where the dredged sediment composition is 50% of sediment particles < 20µm.

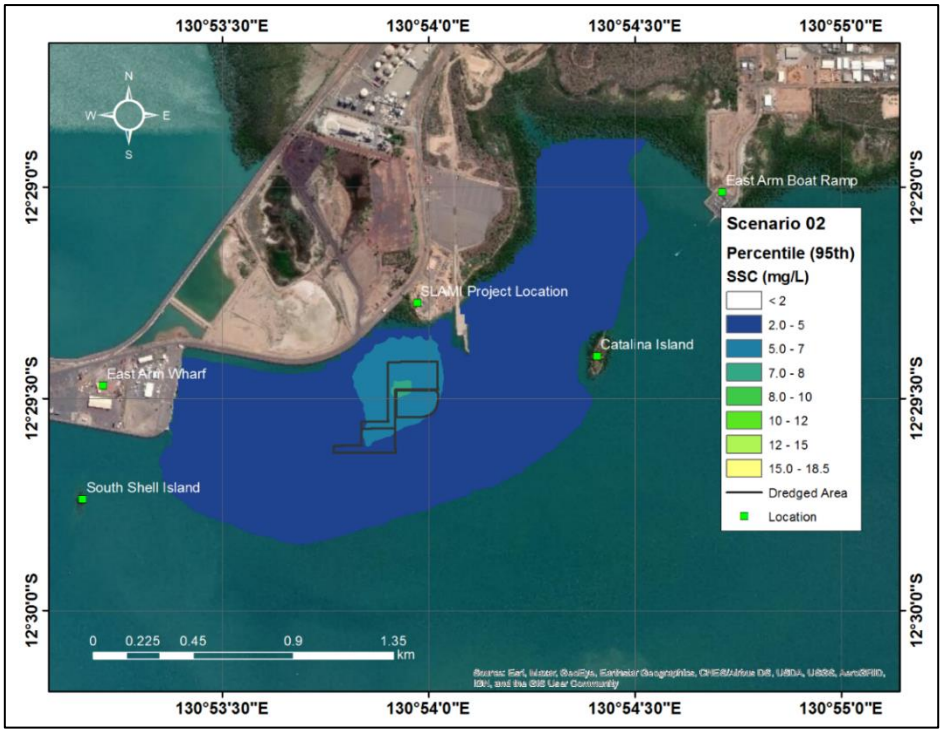

Figure 14: Spatial limits of the area subjected to 95th percentile of SSC in the water column (above background level) based on Scenario 02 where the dredged sediment composition is 30% of sediment particles < 20µm.

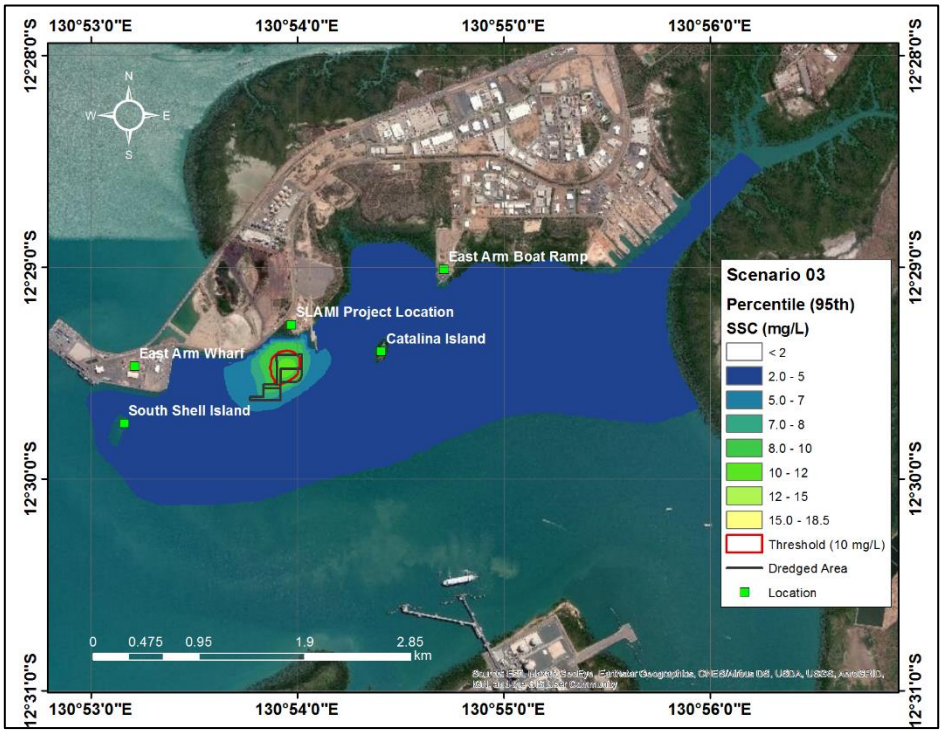

Figure 15: Spatial limits of the area subjected to 95th percentile of SSC in the water column (above background level) based on Scenario 03 where the dredged sediment composition is 50% of sediment particles < 20µm.

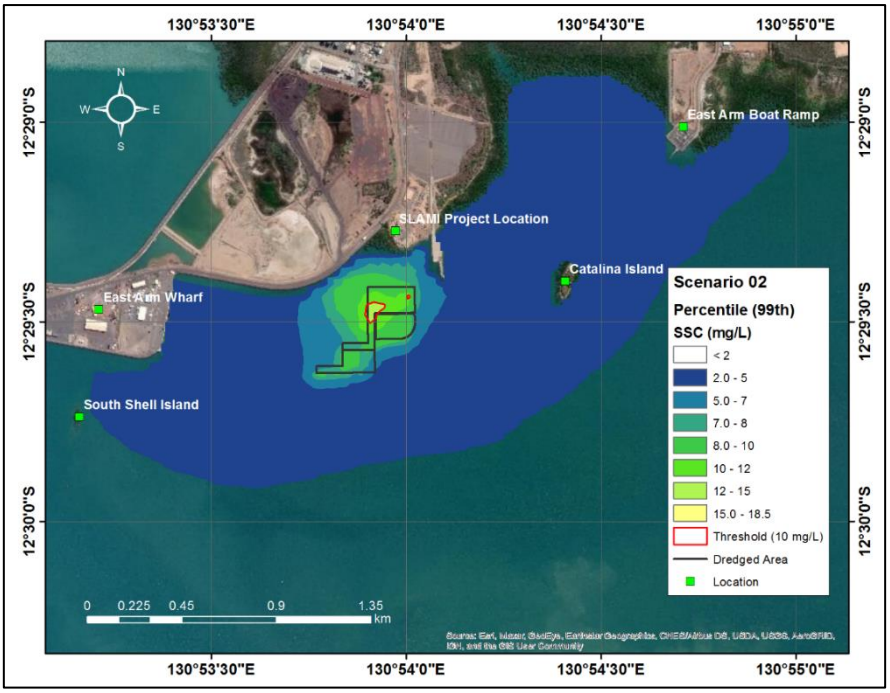

Figure 16: Spatial limits of the area subjected to 99th percentile suspended sediment concentration in the water column (above background level) based on Scenario 02 where the dredged sediment composition is 30% of particles < 20µm.

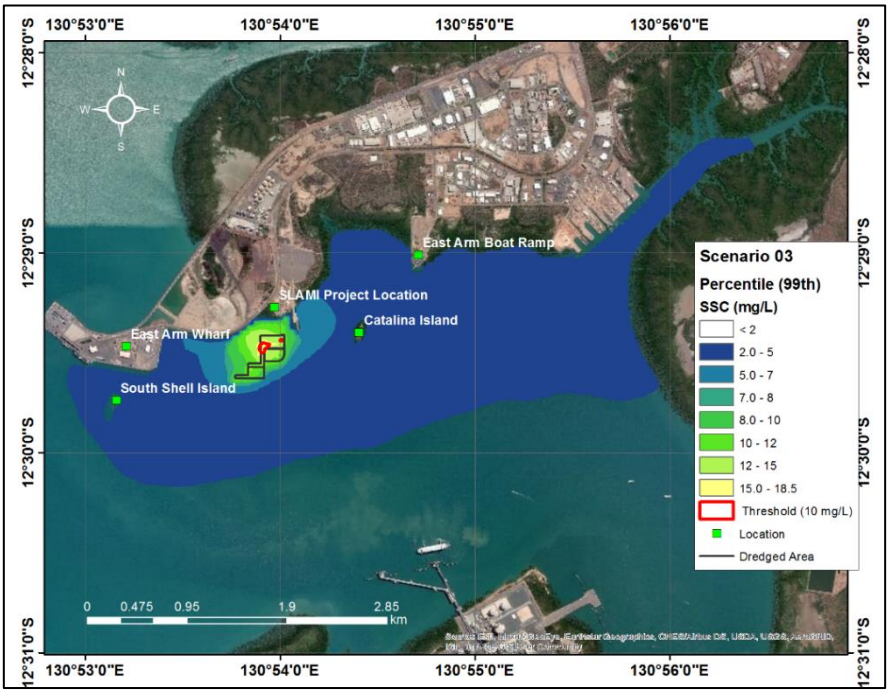

Figure 17: Spatial limits of the area subjected to 99th percentile suspended sediment concentration in the water column (above background level) based on Scenario 03 where the dredged sediment composition is 50% of particles < 20µm.

3.2.2. Temporal behaviour of the sediment plume at dredging locations.

A set of locations in the vicinity of the dredging locations were chosen to assess the temporal behaviour of SSC during dredging operations as simulated by the model (Figure 9).

Results from Scenario 02 showed that the SSC exceeded the threshold of 10 mg/L at points P4, P5 and P6, but these values above the threshold were short lived about 2 hours (Figure 18 and Figure 19). The highest concentration observed was about 24 mg/L at the point P5 (Figure 19). The 25 mg/L threshold was not exceeded anywhere (Figure 18 and Figure 19). The highest SSC observed at P5 would be due to its location, inside of dredging area.

The results obtained by cumulative probability calculations based on the modelling results suggest a low probability (<3% during the period simulated) for SSC to exceed the value of 10 mg/L at points P4, P5 and P6 (Table 5). Outside the dredging area, the model results suggest that the SSC should not exceed the 10 mg/L threshold.

Finally, the Scenario 03 (Figure 20 and Figure 21) presents an increase of the maximum SSC, reaching levels about 27 mg/L at P4 and P5 which is above the threshold of 25 mg/L .

Regards to the exceedance probability (Table 5), the model suggests a low probability (<5% during the period simulated) for SSC to exceed the value of 25 mg/L at P5 and P6. Also, less than 10% of probability of SSC to exceed values of 10 mg/L at P4, P5 and P6.

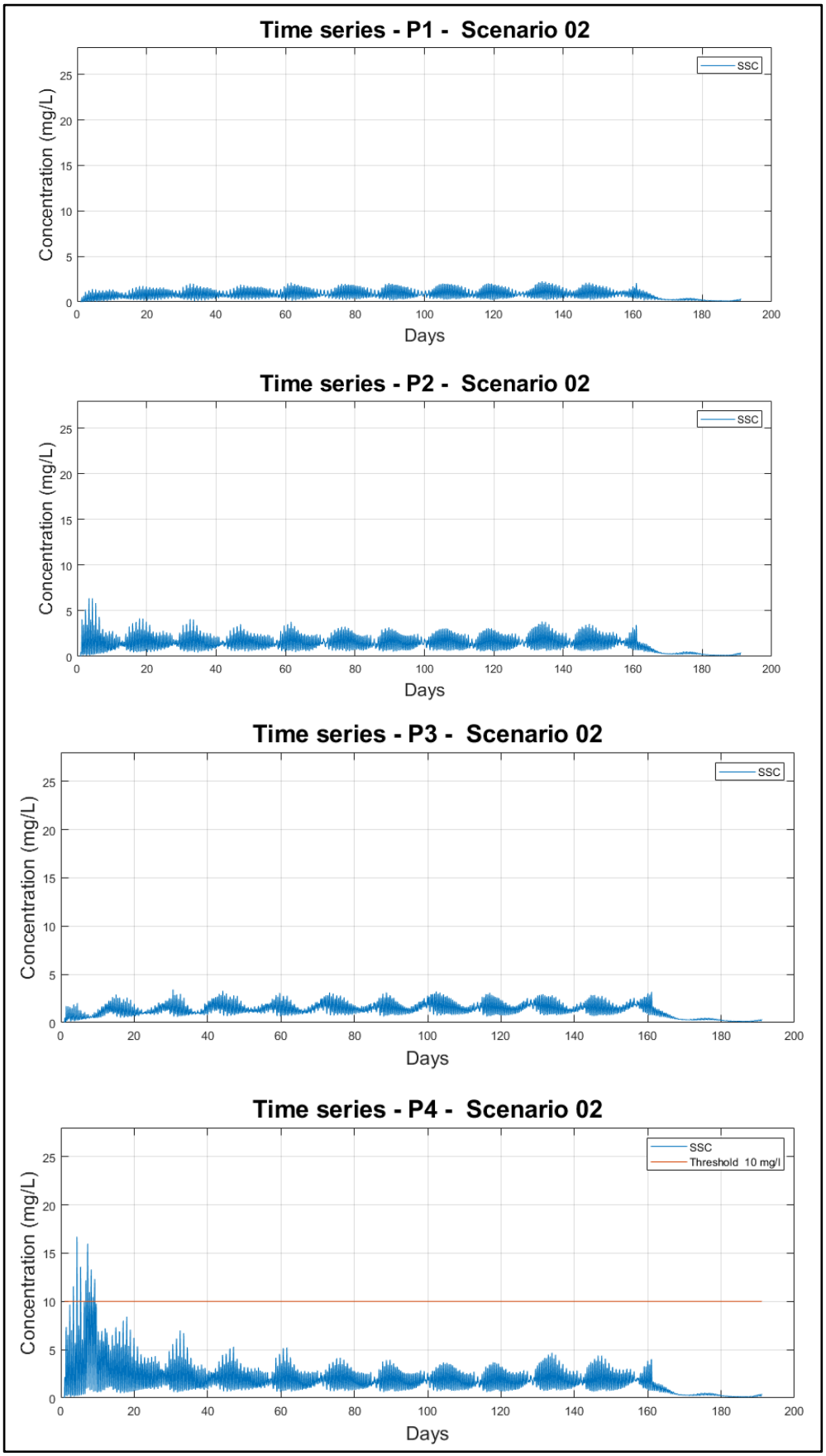

Figure 18: Time series of the maximum SSC (above background level, in mg/L) at P1, P2, P3 and P4, in the water column as result of Scenario 02 numerical modelling.

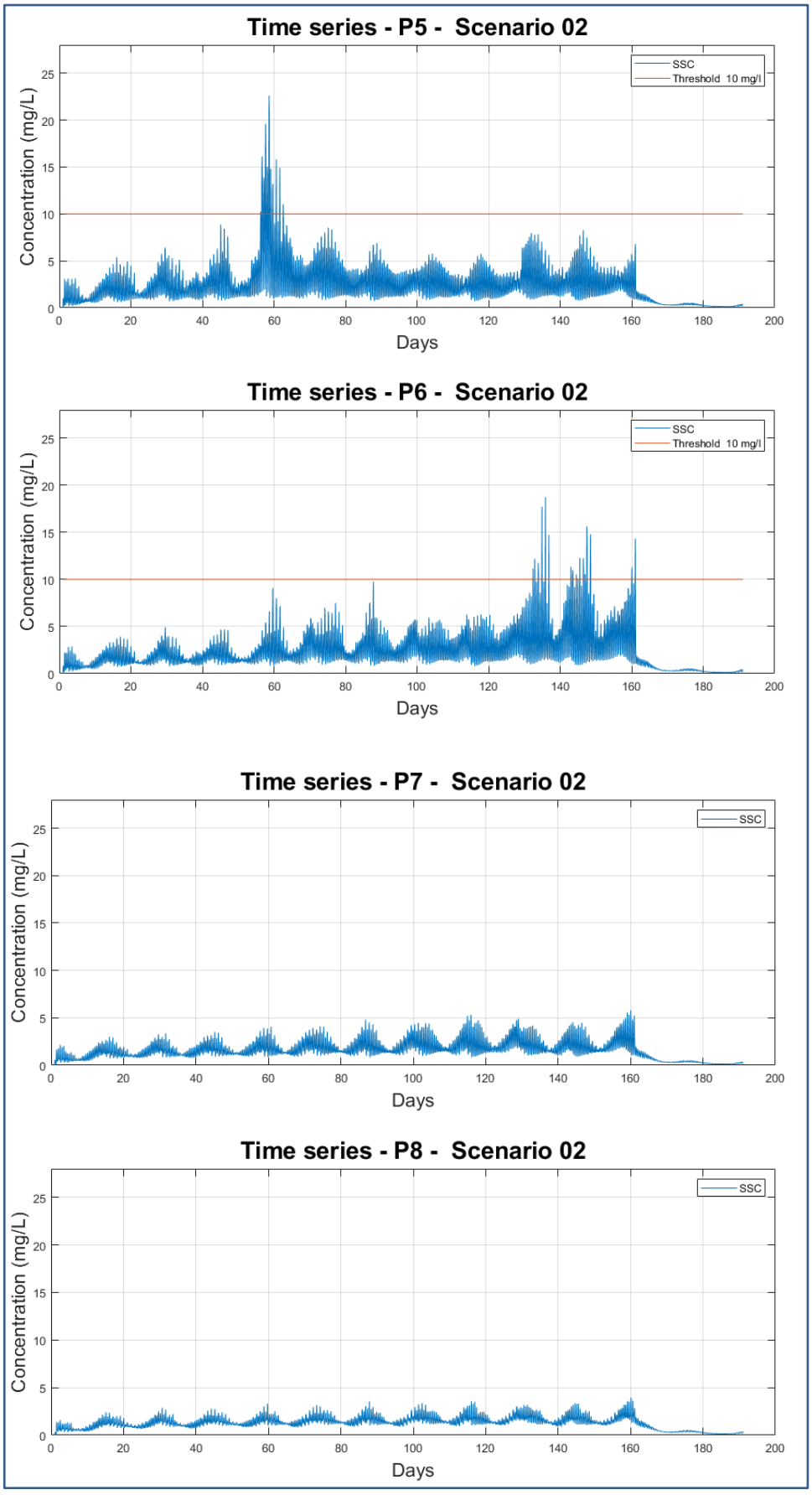

Figure 19: Time series of the maximum SSC (above background level, in mg/L) at P5, P6, P7 and P8, in the water column as result of Scenario 02 numerical modelling**.**

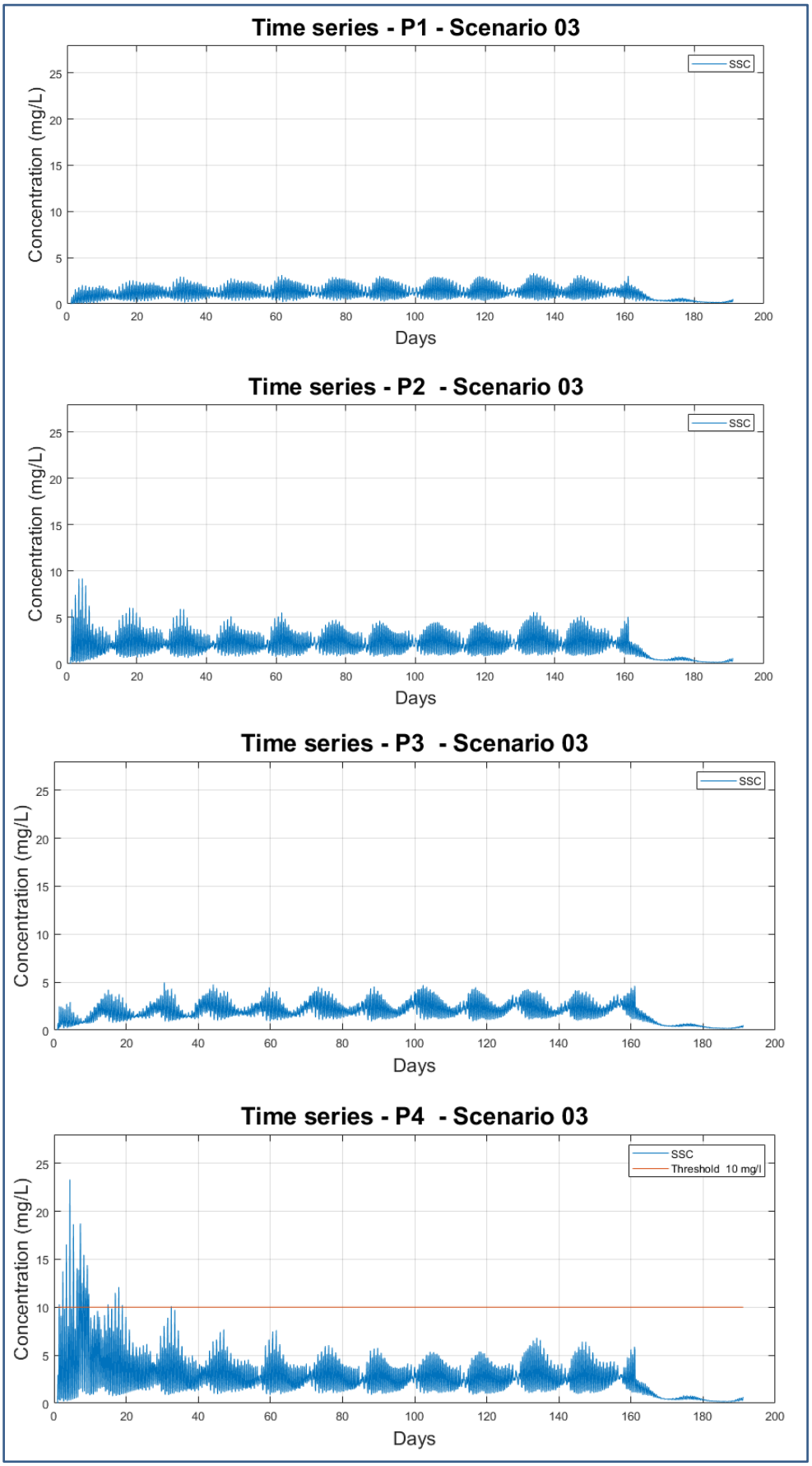

Figure 20: Time series of the maximum SSC (above background level, in mg/L) at P1, P2, P3 and P4, in the water column as result of Scenario 03 numerical modelling.

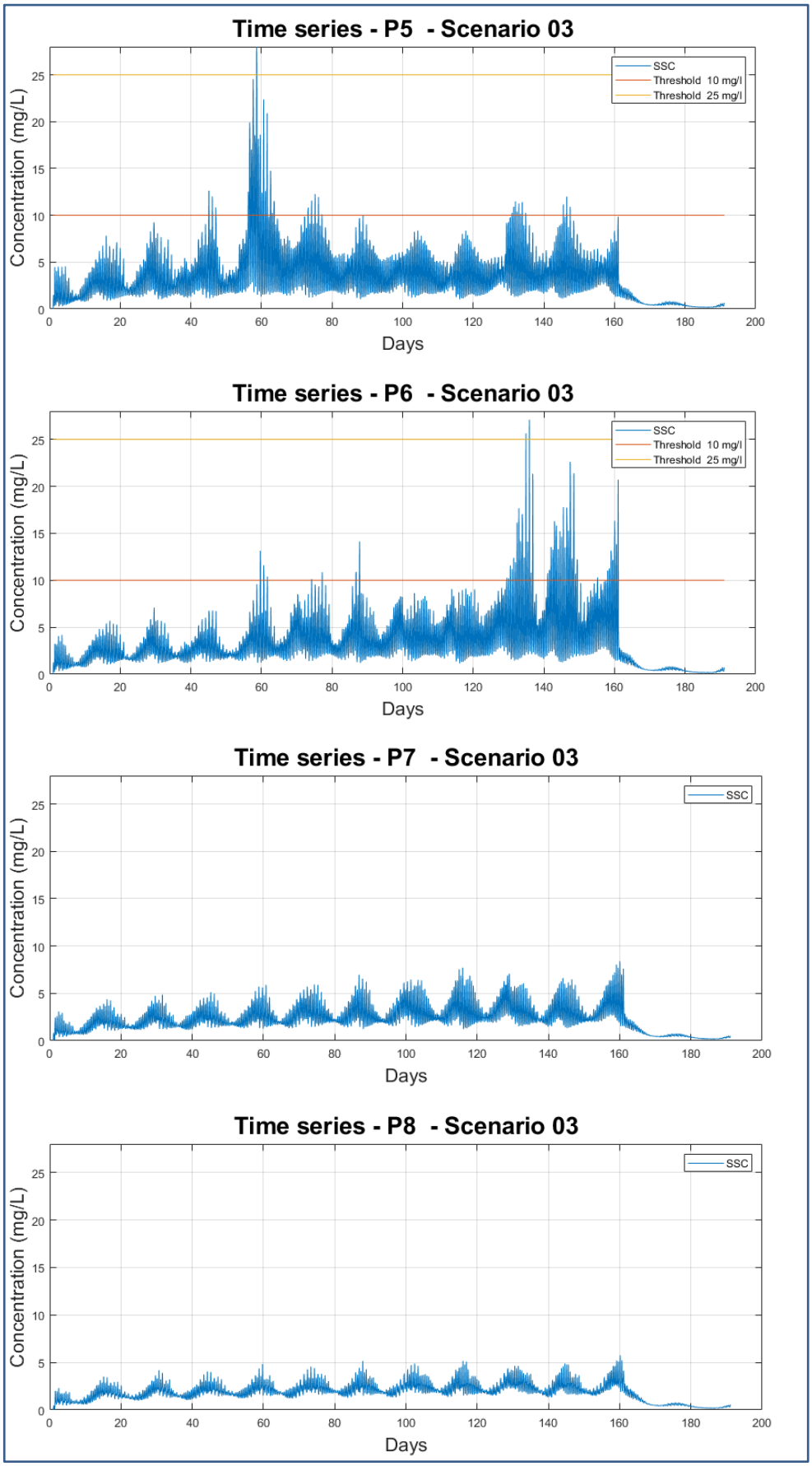

Figure 21: Time series of the maximum SSC (above background level, in mg/L) at P5, P6, P7 and P8, in the water column as result of Scenario 03 numerical modelling.

Table 5: Percentage of the simulated period subject to exceed the specific thresholds according to respective scenarios (period simulated: 23.2 weeks plus 30 days).

Point	Scenario 02	Scenario 03	Scenario 02	Scenario 03
	Probability (%) to exceed 10 mg/L		Probability (%) to exceed 25 mg/L	
P1	0	0	0	0
P2	0	0	0	0
P3	0	0	0	0
P4	2	3	0	0
P5	2	3	0	1
P6	2	5	0	1
P7	0	0	0	0
P8	0	0	0	0

3.2.3. Deposition of sediment during dredging operations

The maximum deposition thickness as result of the numerical modelling at the end of 23.2 weeks of the dredging was 160 mm for the Scenario 02 (Figure 22) and 130 mm for the Scenario 03 (50% fine sediment increase) (Figure 23).

The deposition of sediment, as consequence of the dredging operations, was not limited to the region close to the boundaries of dredging polygon (Figure 17). It is possible to observe areas subject to deposition with thickness less than 10mm in distances around 50m outside the limits of the dredging polygon (Figure 17).

Four different classes of sediment (gravel, sand, silt and clay) were used in the simulations. The high thickness surrounding the dredging area (Figure 22 and Figure 23) is associated with the PSD. The coarse material tends to be deposited in the region of dredging polygon and surroundings (high thickness), mainly due the low mean current velocity (<0.3 m/s). The fine material, which is easily advected by the currents (due to its low settling velocity) tends to be deposited away from the dredging area (small thickness).

As the fine sediment has a higher capacity to be advected by the current, the Scenario 03 presents sediment deposition in different areas compared to the Scenario 02. In the Scenario 03 the results suggest that areas far from the dredging location such as South Shell Island can be slightly more affected by the dredging activity if we consider an increase of the fine sediment in 50%.

Although the region surrounding the boundaries of the dredging polygon are where the highest sediment deposition occurs, other parts of the East Arm, such as nearby the East Arm Boat Ramp, will experience low levels of sediment deposition based on the numerical model predictions in both scenarios.

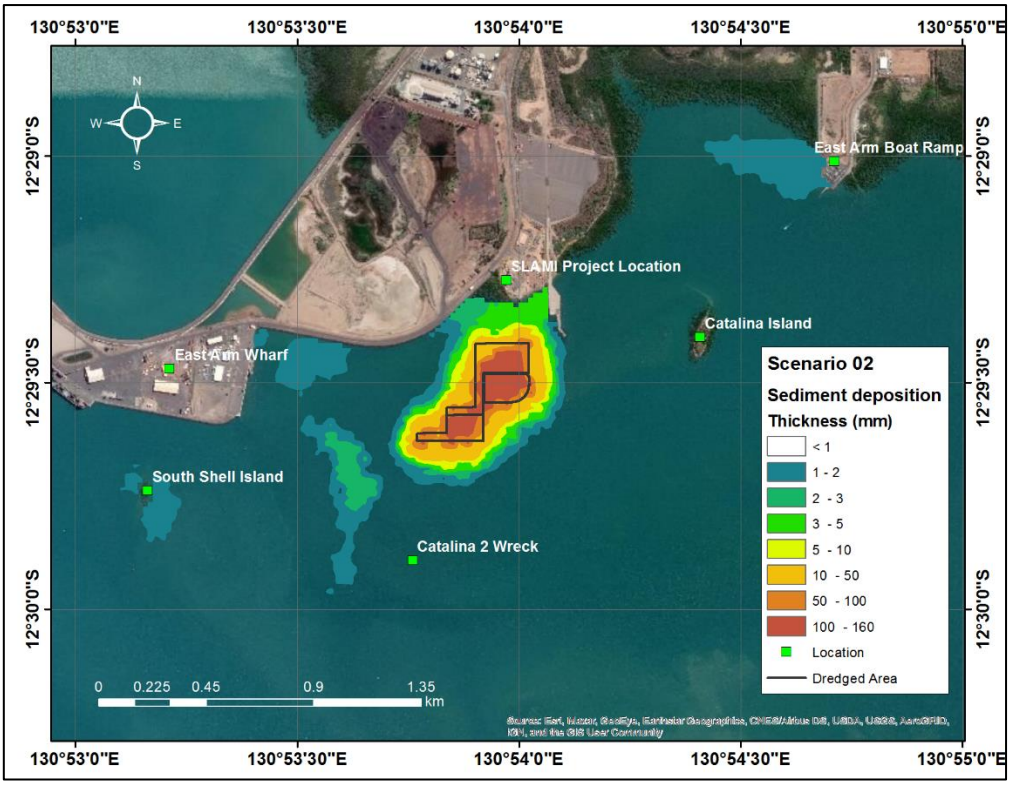

Figure 22: Primary sediment deposition thickness (in mm) on the seabed at the end of the entire dredging program (result of numerical modelling). The duration of entire dredging program was 23.2 weeks plus 30 days for assessment after the sediment source has ceased (Scenario 02).

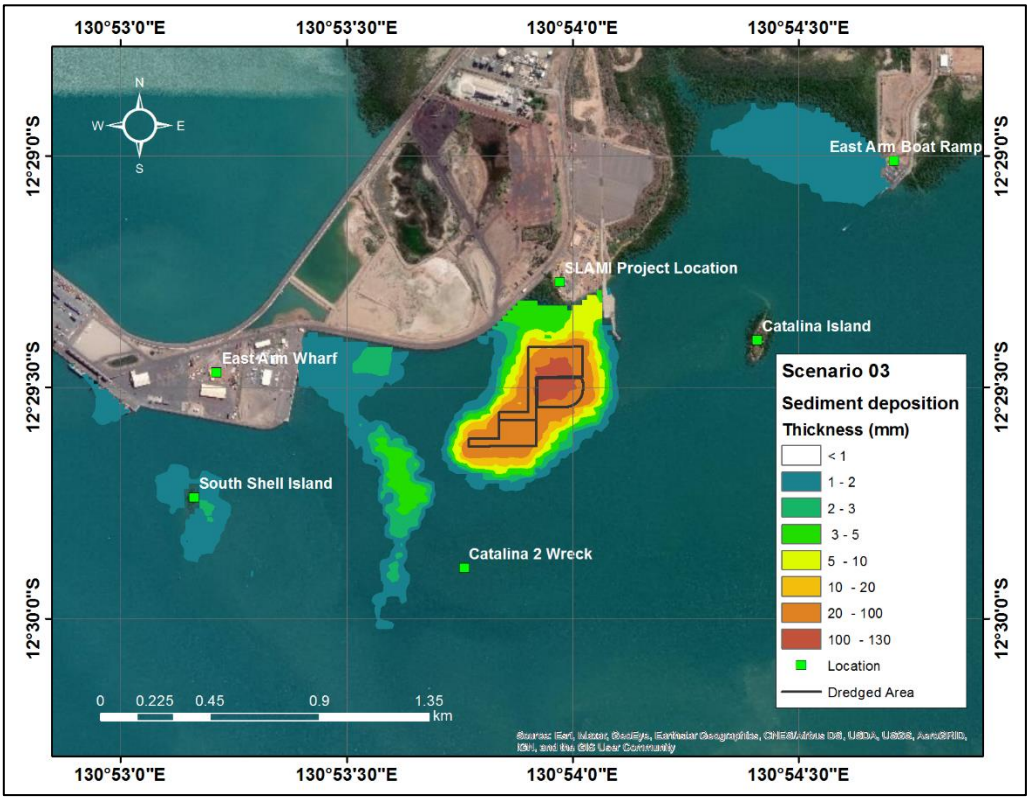

Figure 23: Primary sediment deposition thickness (in mm) on the seabed at the end of the entire dredging program (result of numerical modelling). The duration of entire dredging program was 23.2 weeks plus 30 days for assessment after the sediment source has ceased (Scenario 03).

3.2.4. Deposition and Removal rate of sediment during dredging operations

The observation points (Figure 9) were used by the model to register the process of deposition and removal rate of sediments originating from the dredging operation and did not include natural sediment transport in the area. The interval of about 14 days between the maximum (minimum) peaks of deposition/removal rates observed at all monitored sites suggests that the tide cycle has an important role in that process (Figures 24 to 39). The maximum sediment deposition rates occur during neap tides (less energetic local currents induced by tides) and the maximum removal rates occurs during spring tides (more energetic local currents induced by tides). The model results showed the deposition and removal rate are also associated with the position of the site in relation to the dredging region (Figures 24 to 39).

The points P1, P2, P3, P7 and P8 have low deposition rates compared to P4, P5 and P6 (Figures 24 to 39) the deposited sediment at these sites are possibly mainly composed of fine sediments (silt and clay), since the lighter sediment is transported away from its origin by local currents. The points P4, P5 and P6, located within the proposed dredging footprint, have a higher deposition rate, likely to be associated with the coarse material (sand and gravel).Due to the low current velocity associated with those locations the removal rate at P4, P5 and P6 is very low compared to the deposition.

The observed difference between Scenario 02 and 03 is that in the Scenario 03 the deposition rate is about 50% higher than the Scenario 02 especially at point the P1. The maximum observed deposition rate in the Scenario 02 at P1 is 0.008 (mm/h) and in the Scenario 03 at P1 is 0.012 (mm/h).

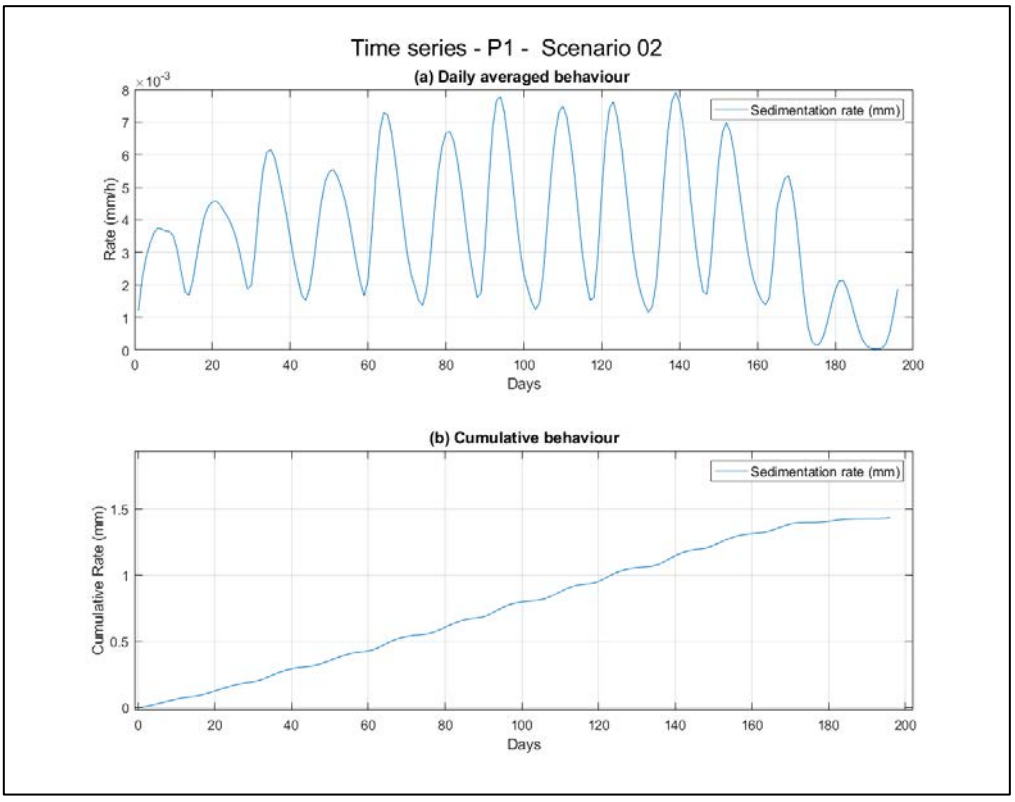

Figure 24: Time series of sediment deposition and removal rate (in mm/h, top panel) and time series of cumulative behaviour (in mm, bottom panel) for point 1 under Scenario 02 modelling. Positive values represent deposition rate and negative values represent removal rate.

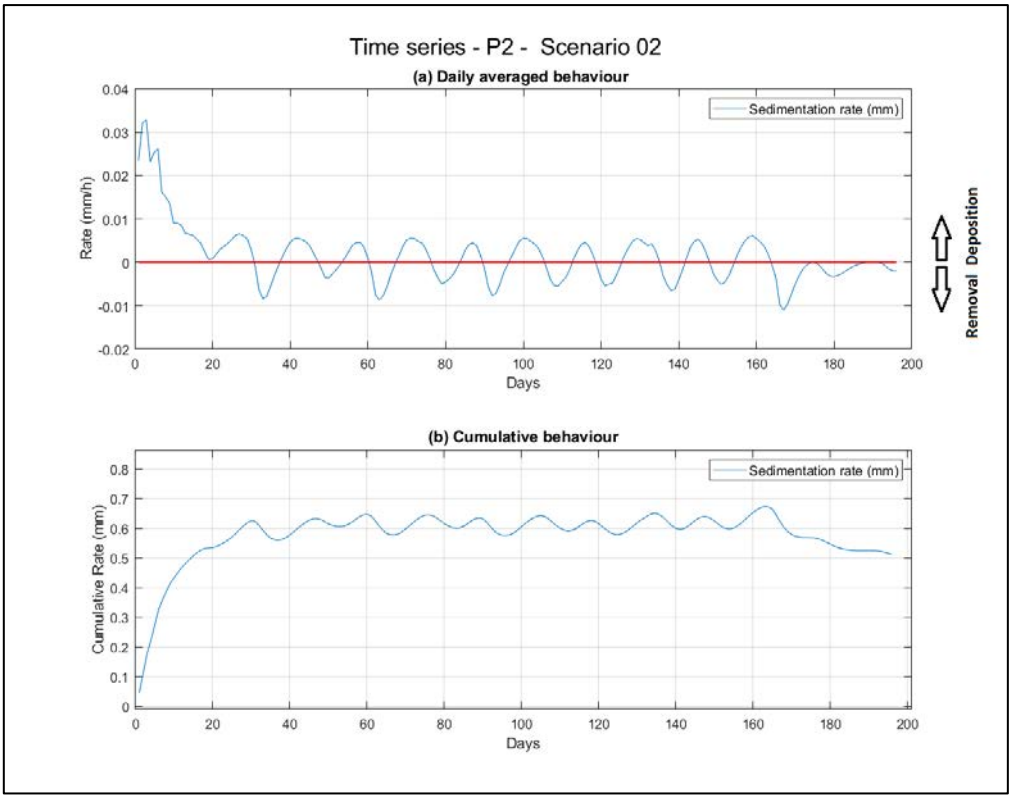

Figure 25: Time series of sediment deposition and removal rate (in mm/h, top panel) and time series of cumulative behaviour (in mm, bottom panel) for point 2 under Scenario 02 modelling. Positive values represent deposition rate and negative values represent removal rate.

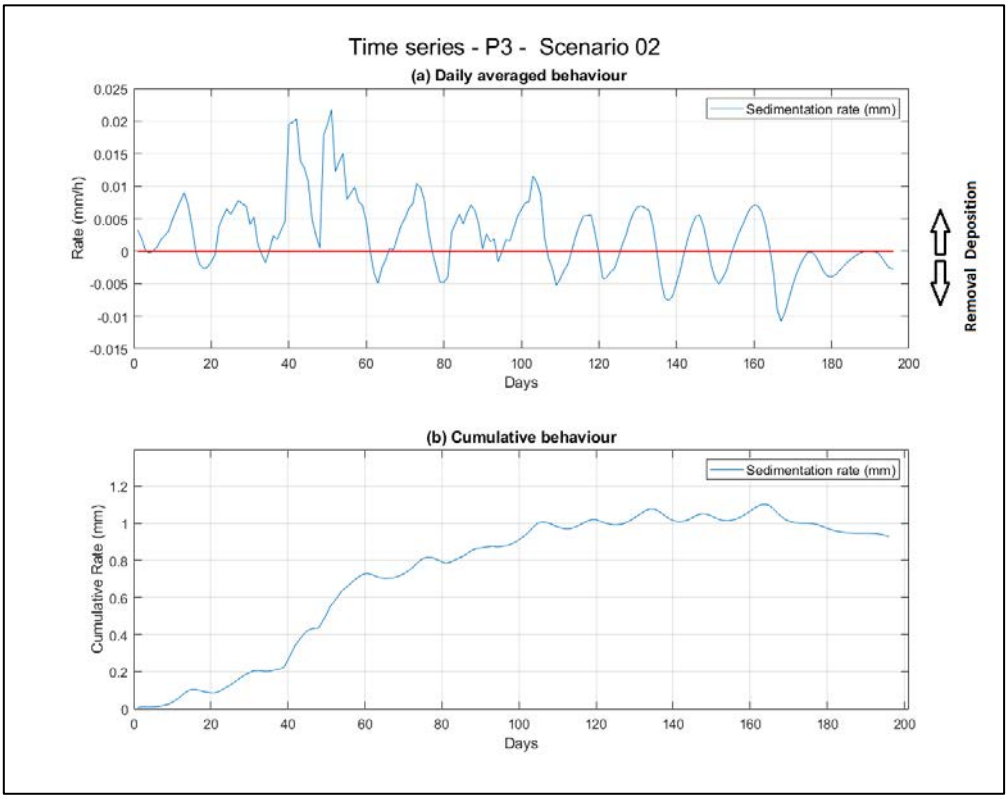

Figure 26: Time series of sediment deposition and removal rate (in mm/h, top panel) and time series of cumulative behaviour (in mm, bottom panel) at point 3 under Scenario 02. Positive values represent deposition rate and negative values represent removal rate.

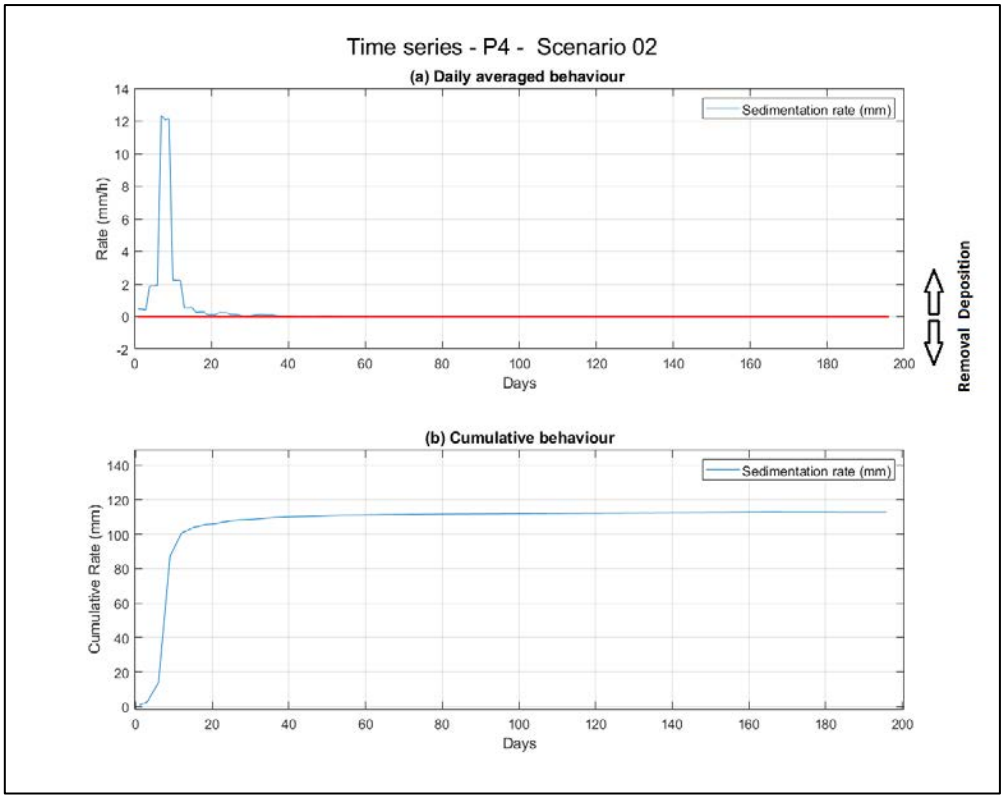

Figure 27: Time series of sediment deposition and removal rate (in mm/h, top panel) and time series of cumulative behaviour (in mm, bottom panel) at point 4 under Scenario 02. Positive values represent deposition rate and negative values represent removal rate.

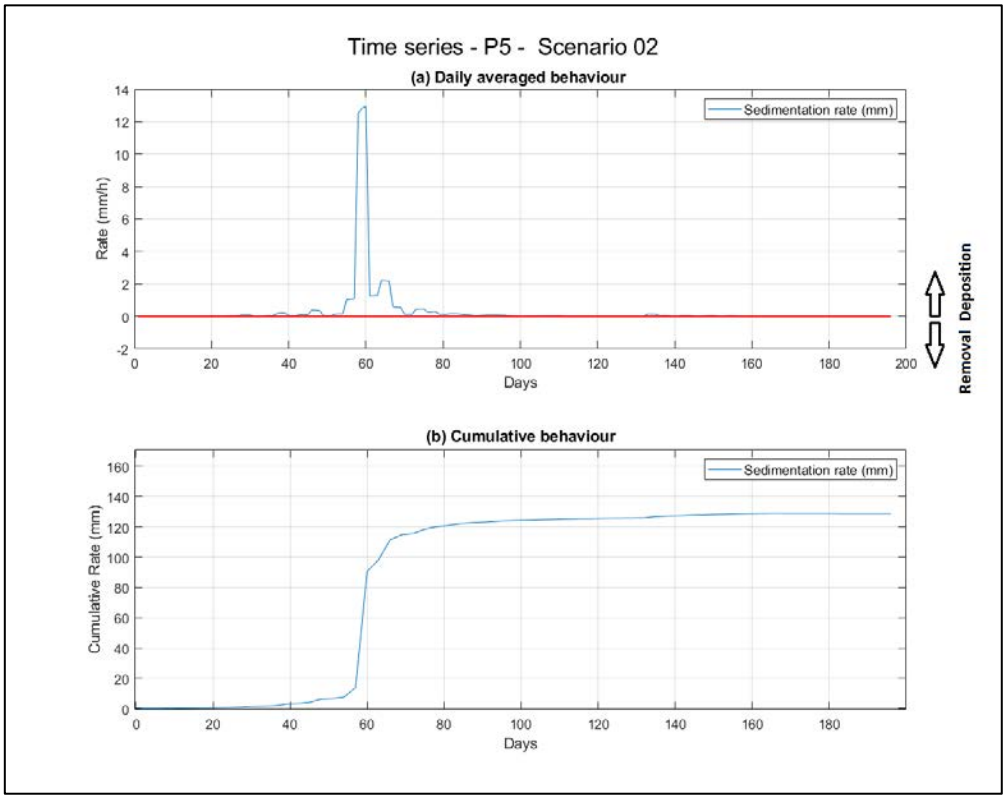

Figure 28: Time series of sediment deposition and removal rate (in mm/h, top panel) and time series of cumulative behaviour (in mm, bottom panel) at point 5 under Scenario 02. Positive values represent deposition rate and negative values represent removal rate.

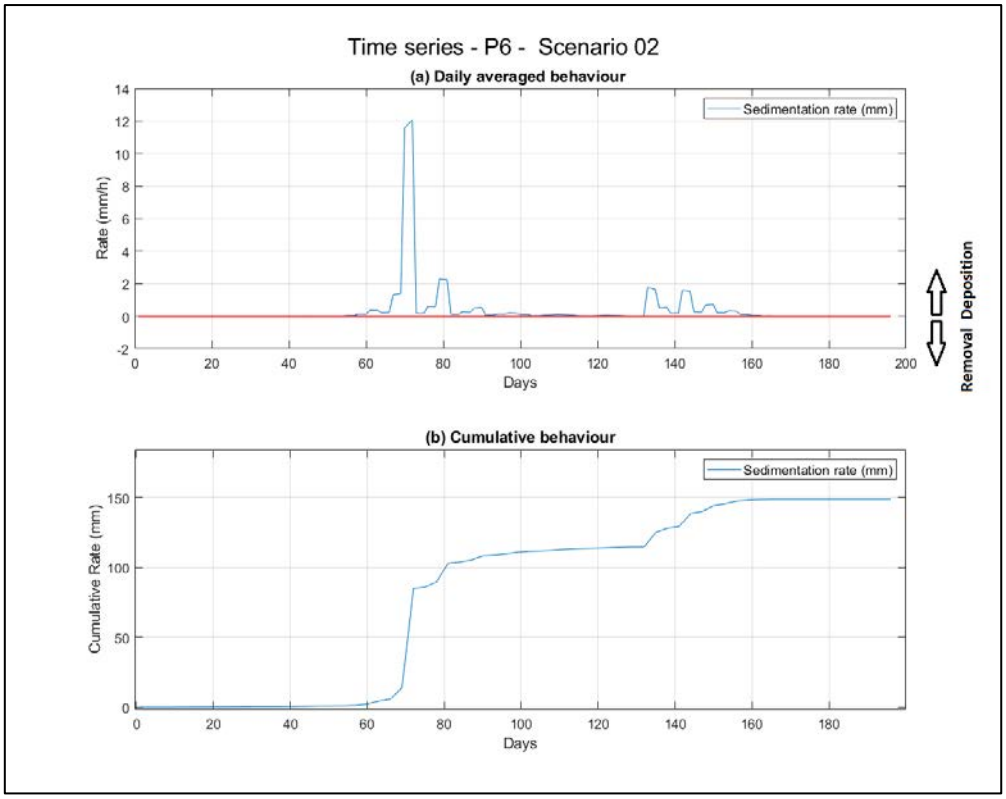

Figure 29: Time series of sediment deposition and removal rate (in mm/h, top panel) and time series of cumulative behaviour (in mm, bottom panel) at point 6 under Scenario 02. (Scenario 02). Positive values represent deposition rate and negative values represent removal rate.

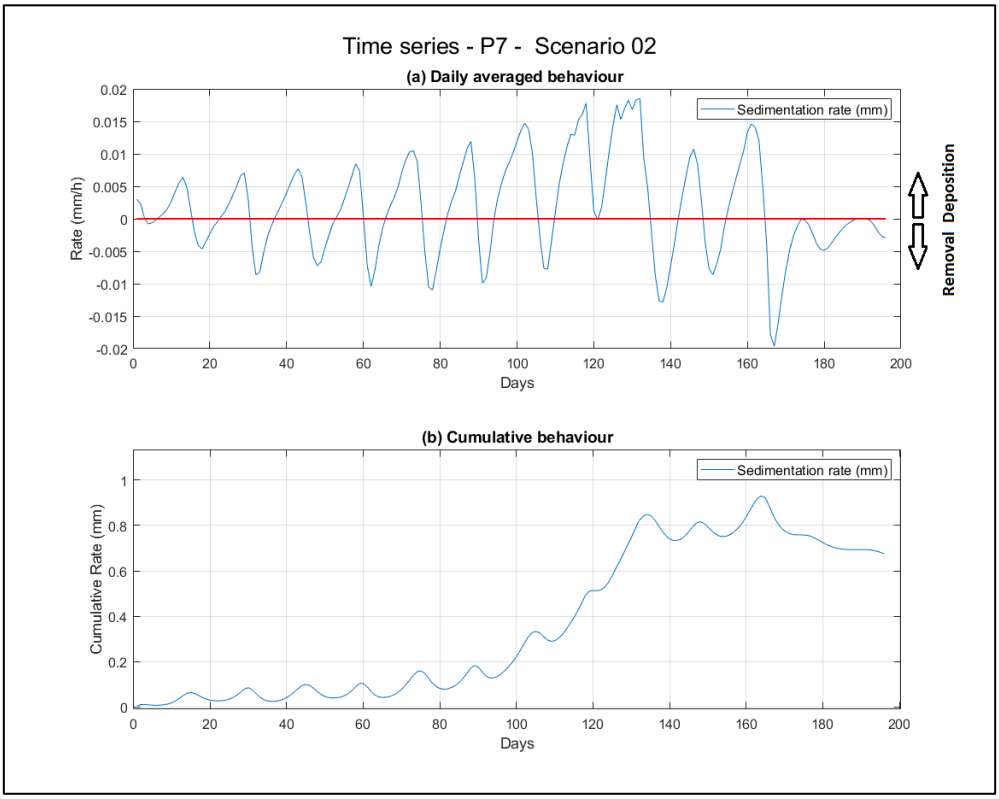

Figure 30: Time series of sediment deposition and removal rate (in mm/h, top panel) and time series of cumulative behaviour (in mm, bottom panel) at point 7 under Scenario 02. Positive values represent deposition rate and negative values represent removal rate.

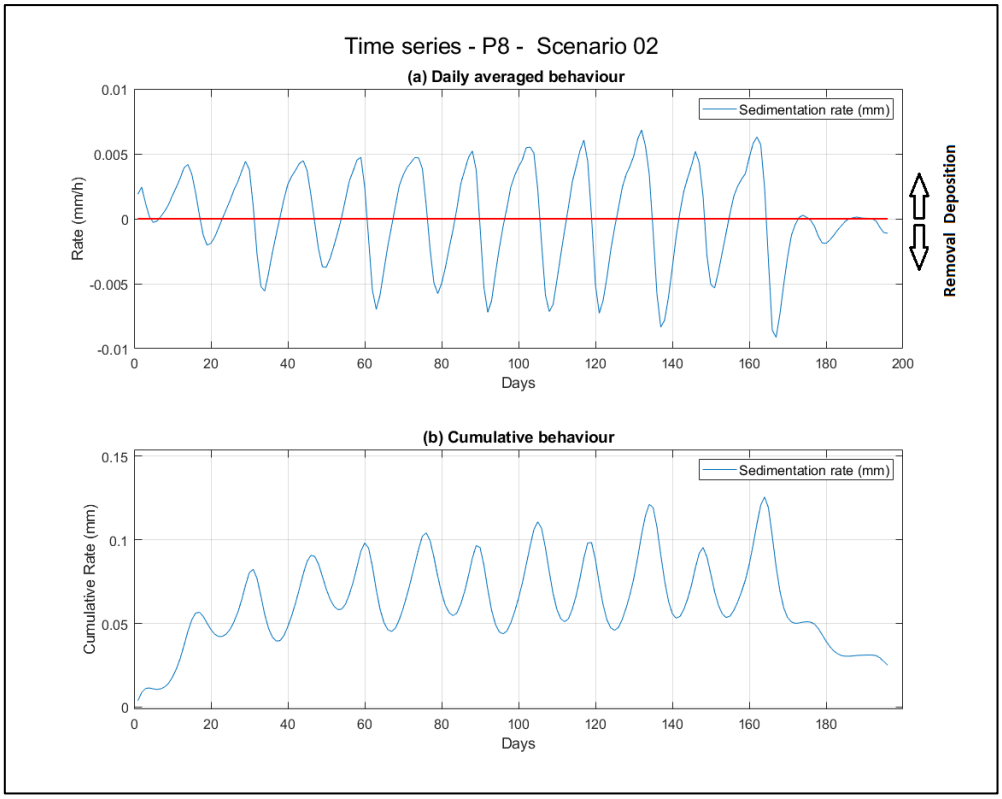

Figure 31: Time series of sediment deposition and removal rate (in mm/h, top panel) and time series of cumulative behaviour (in mm, bottom panel) at point 8 under Scenario 02. Positive values represent deposition rate and negative values represent removal rate.

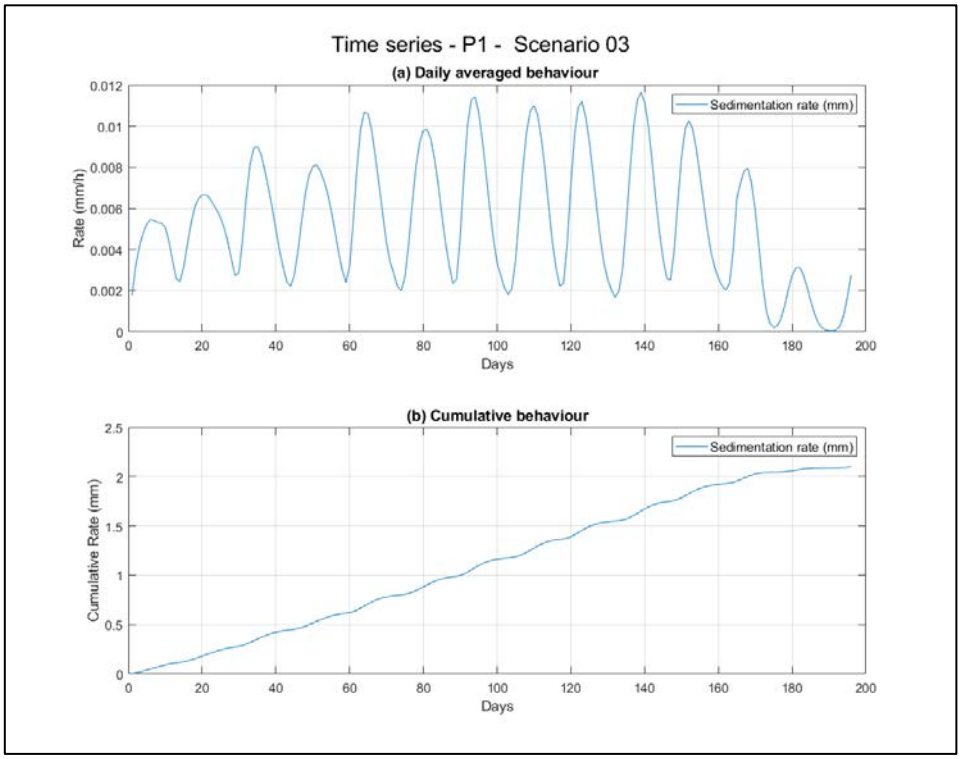

Figure 32: Time series of sediment deposition and removal rate (in mm/h, top panel) and time series of cumulative behaviour (in mm, bottom panel) at point 1 under Scenario 03. Positive values represent deposition rate and negative values represent removal rate.

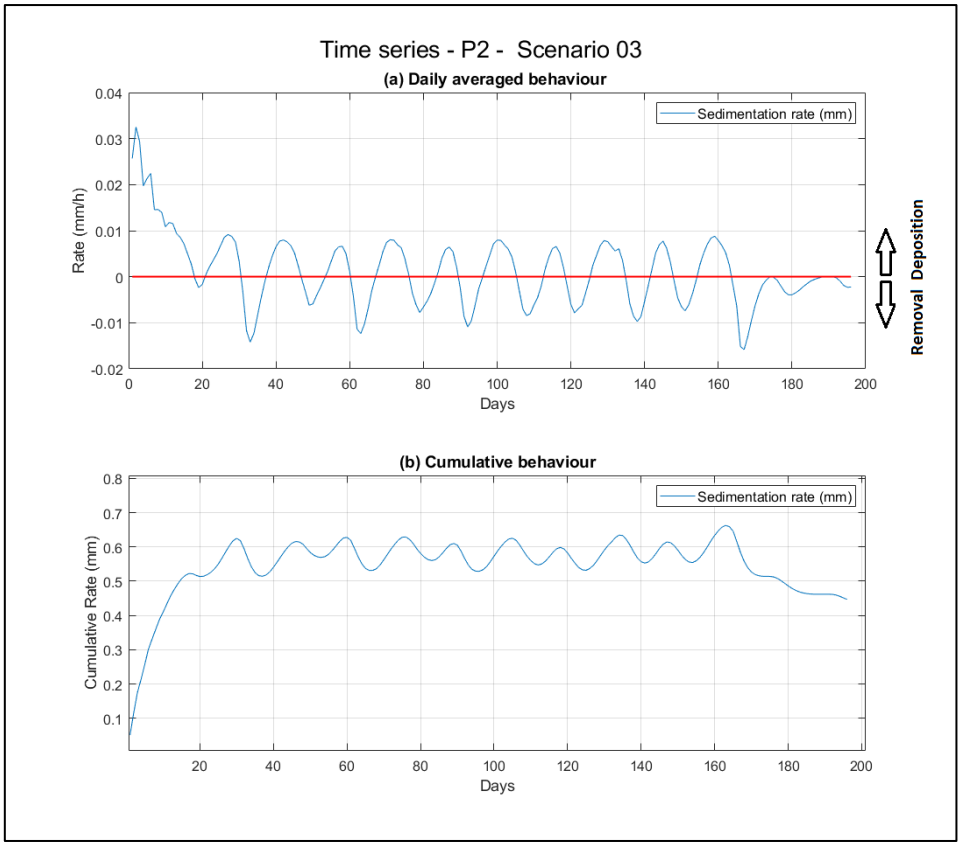

Figure 33: Time series of sediment deposition and removal rate (in mm/h, top panel) and time series of cumulative behaviour (in mm, bottom panel) at point 2 under Scenario 03. Positive values represent deposition rate and negative values represent removal rate.

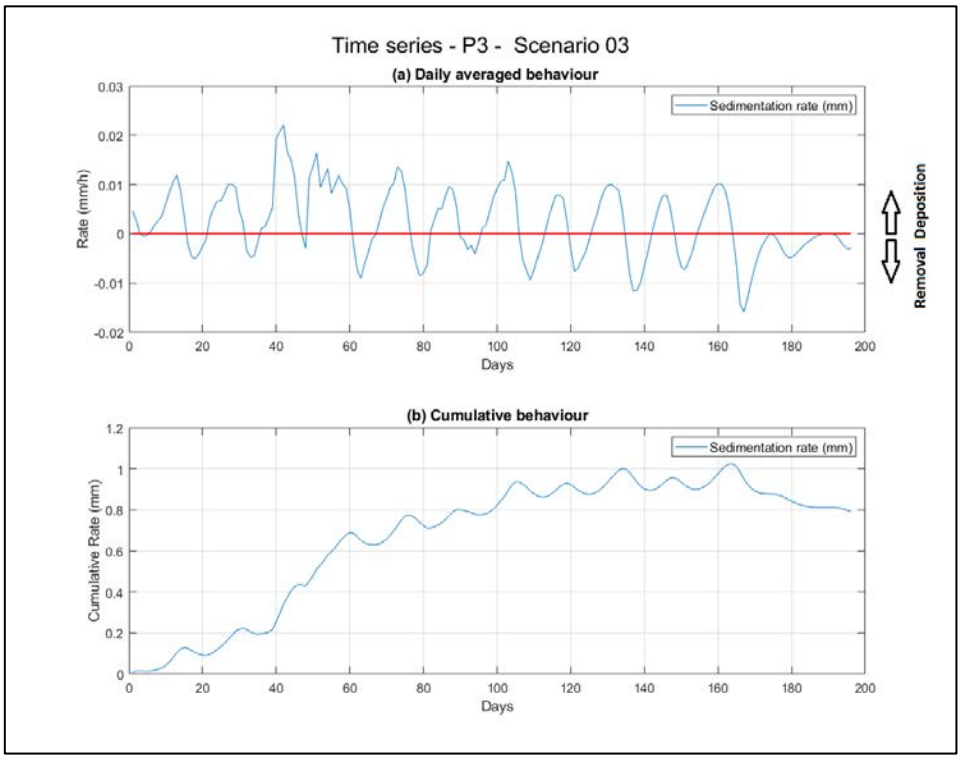

Figure 34: Time series of sediment deposition and removal rate (in mm/h, top panel) and time series of cumulative behaviour (in mm, bottom panel) at point 3 under Scenario 03. Positive values represent deposition rate and negative values represent removal rate.

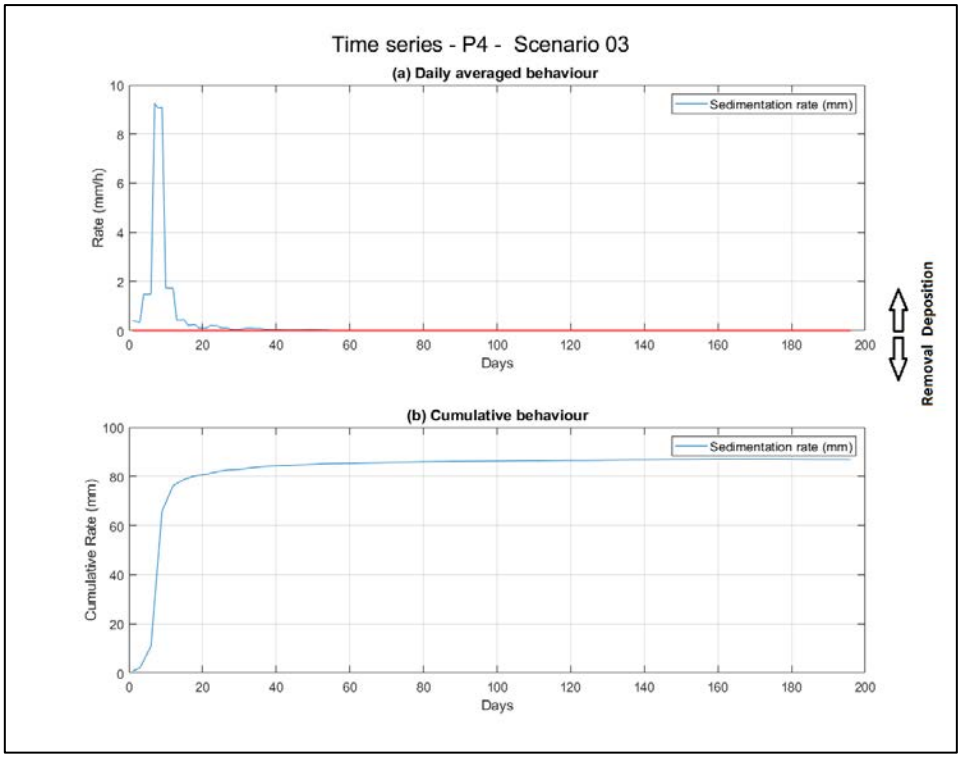

Figure 35: Time series of sediment deposition and removal rate (in mm/h, top panel) and time series of cumulative behaviour (in mm, bottom panel) at point 4 under Scenario 03. Positive values represent deposition rate and negative values represent removal rate.

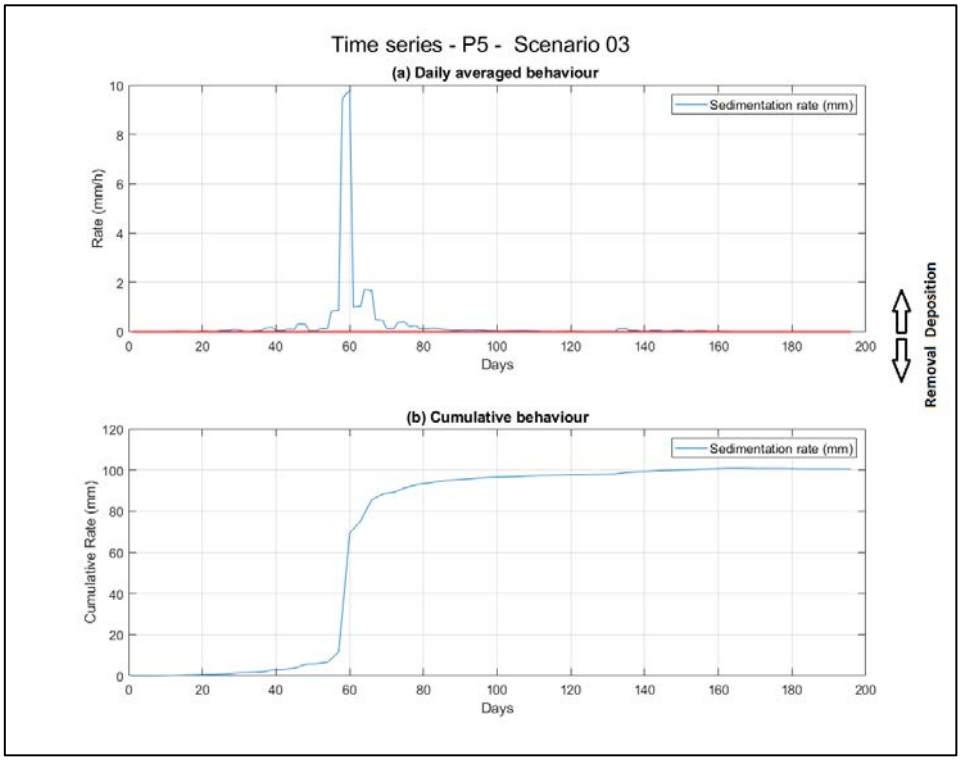

Figure 36: Time series of sediment deposition and removal rate (in mm/h, top panel) and time series of cumulative behaviour (in mm, bottom panel) at point 5 under Scenario 03. Results from numerical modelling for point P5. Positive values represent deposition rate and negative values represent removal rate.

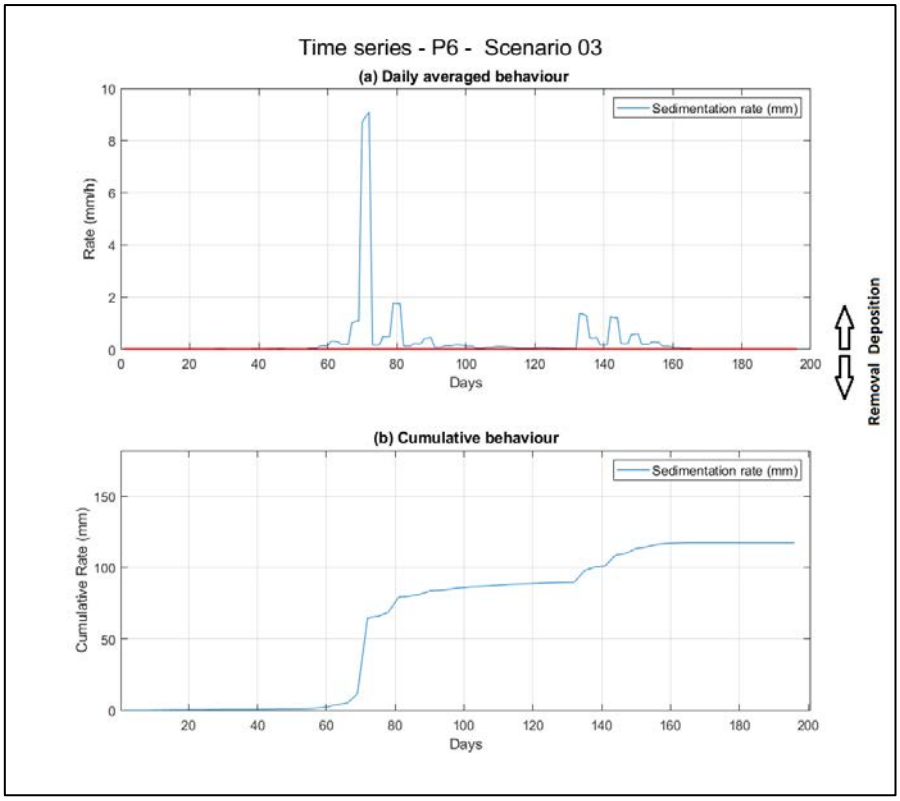

Figure 37: Time series of sediment deposition and removal rate (in mm/h, top panel) and time series of cumulative behaviour (in mm, bottom panel) at point 6 under Scenario 03. Positive values represent deposition rate and negative values represent removal rate.

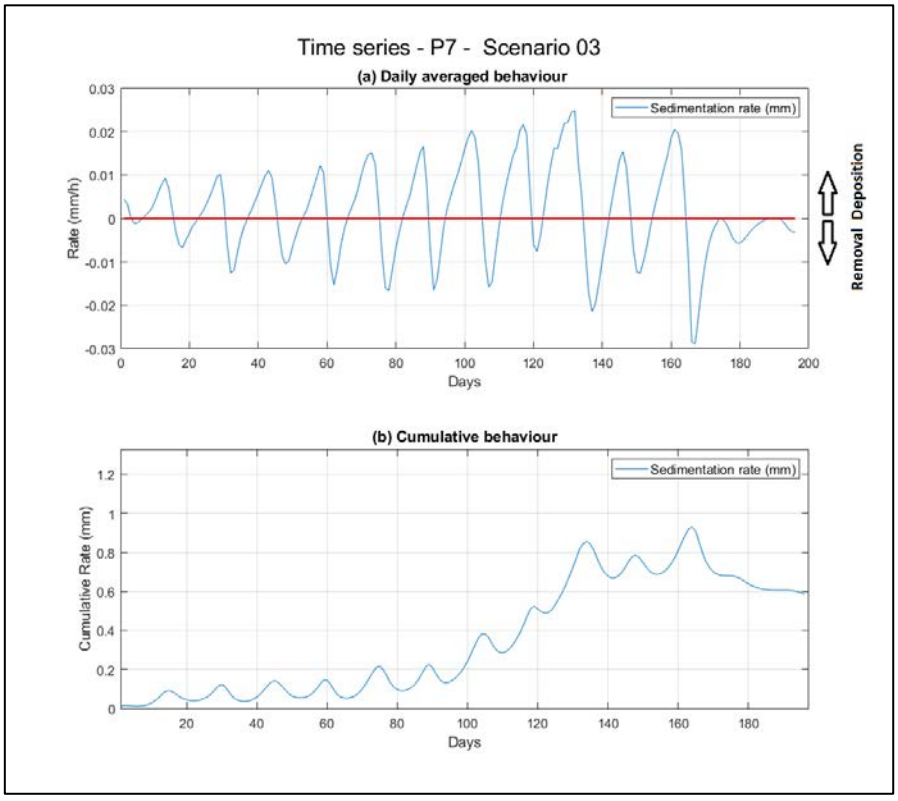

Figure 38: Time series of sediment deposition and removal rate (in mm/h, top panel) and time series of cumulative behaviour (in mm, bottom panel) at point 7 under Scenario 03. Positive values represent deposition rate and negative values represent removal rate.

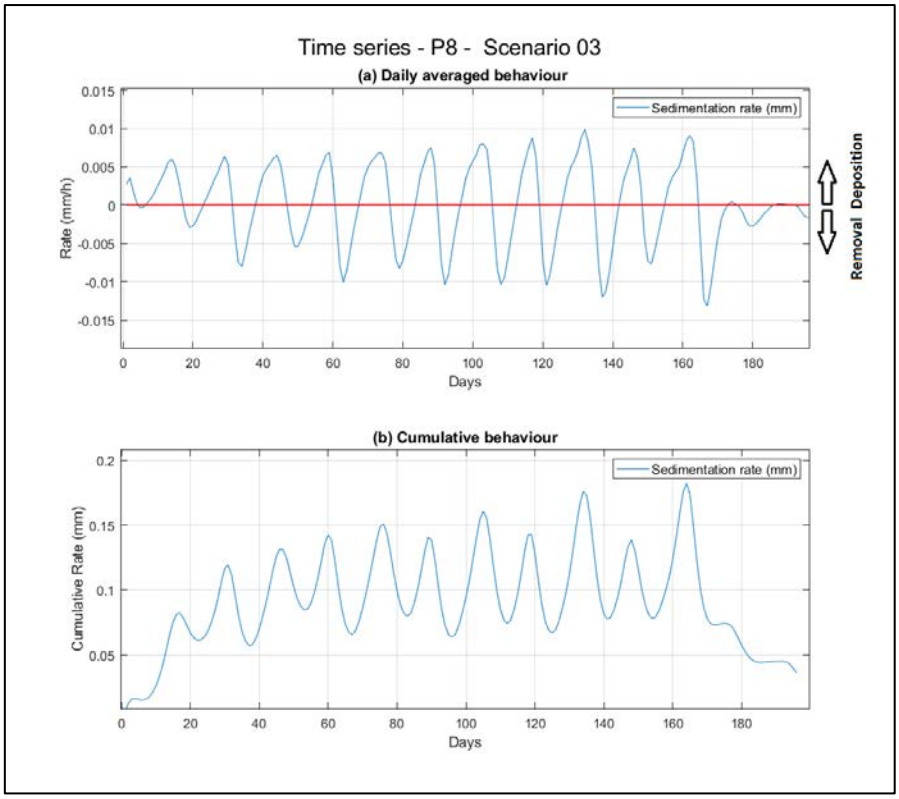

Figure 39: Time series of sediment deposition and removal rate (in mm/h, top panel) and time series of cumulative behaviour (in mm, bottom panel) at point 8 under Scenario 03. Positive values represent deposition rate and negative values represent removal rate.

4. SUMMARY OF NUMERICAL MODELLING OF DREDGING OPERATIONS

The results of the numerical modelling of the dredging operations of the Darwin Ship Lift project suggest:

Predicted SSC Scenario 02:

- For Scenario 02 elevated SSC levels are locally restricted to the dredging activities.
- SSC concentrations are predicted to rarely exceed 10 mg./L above background (<5% of the time) and the exceedances are short lived.
- SSC values were not predicted to exceed the 25 mg/L threshold in any location under Scenario 02 modelling.

Predicted sedimentation Scenario 02:

- Sediment deposition was highest in the dredging footprint area.
- Outside of the proposed dredging footprint the maximum sedimentation deposition rate is less than 0.16 mm/h.
- Sediment deposition at sites far from the dredging area is likely associated with fine sediment.

Predicted SSC Scenario 03:

- Despite an increase of fine sediment in the Scenario 03, elevated levels of SSC are restricted to the dredging footprint area.
- Scenario 03 modelling results indicate SSC concentrations will exceed the 10mg/L threshold (above background) for 5% of the simulated period (approximately 6 days). However, they are not sustained at concentrations above the threshold for an extended period of time.
- SSC values have only 1% of probability predicted to exceed the 25 mg/L.

Predicted sedimentation SSC Scenario 03:

- Sediment deposition under Scenario 03 was highest within the dredge footprint area which is consistent with Scenario 02 modelling.
- The maximum sediment deposition rate was 0.2 mm/h for Scenario 03 which is slightly higher than the rate for Scenario 02 (0.16mm/h) at the same location.
- Under Scenario 03, which modelled sediment with higher fines content compared to Scenario 02, the size of the area experiencing sediment deposition and thickness of deposited sediment was slightly higher than Scenario 02. Thus, higher fine sediment in the dredged sediment causes an increase in the spatial extent of the area influenced by elevated SSC concentrations and deposition.

Final Comments

Sediment transport in Darwin Harbour is controlled by the tidally dominated hydrodynamics, and the underpinning hydrodynamic model used in this study has been validated against field observations. Modelling sediment transport is non-trivial, and the sediment transport model has a number of approximations, assumptions and limitations that are relevant when interpreting the modelling results. These are summarized as follows:

- The SSC predicted by the model is not validated and in the Scenario 01 it is only compared qualitatively with other studies.
- The resuspension threshold values are based on values for similar materials from the literature and they may differ from field measurements. The background SSC calculated by the model (Scenario 01) has been qualitatively assessed against previous studies, but the sensitivity of SSC to resuspension threshold values has not been assessed.
- The model had the objective to represent the average condition, consequently extreme scenarios such as cyclones were disregard.
- Waves are not considered in this study due to the study location which is relatively protected from the significative sea (wind waves) or swells.
- Currents driven by tides are the only forcing considered in this study which is responsible for the sediment resuspension observed in the Scenario 01.
- The total area of influence of the activity can be affected proportionally by the concentration of fine sediment dredged.
- All simulation of Scenario 02 and 03 represent the far-field plume behavior.

5. REFERENCES

Australian Institute of Marine Science (2020). Northern Australia Automated Marine Weather and Oceanographic Stations, Sites: [Darwin]. https://doi.org/10.25845/5c09bf93f315d, accessed 16-Sep-2020

Andutta F.P.; Wang X.H.; Li L.; Williams D (2013) Hydrodynamics and Sediment Transport in a Macro-Tidal Estuary: Darwin Harbour, Australia; Springer: Dordrecht, The Netherlands, 2013; pp. 111–129

Brinkman R. and Logan M (2019) Sediment Quality Sampling Design for Darwin Harbour. Reportprepared for Northern Territory Government, Department of Environment and Natural Resources.Australian Institute of Marine Science, Townsville. (110 pp)

Li L. (2013) Modelling the Tidal and Sediment Dynamics in Darwin Harbour, Northern Territory, Australia. Ph.D. Thesis, The University of New South Wales, Canberra, Australia

Siwabessy P.J.W., Tran M., Huang Z., Nichol S., Atkinson I (2015) Mapping and Classification of Darwin Harbour Seabed. Record 2015/18. Geoscience Australia, Canberra. doi:10.11636/Record.2015.018.

Patterson R.G. and Williams D.K. (2014) Sediment transport and bed material testing to support the Darwin Harbour sediment transport model. Report for Land Development Corporation. Australian Institute of Marine Science, Darwin.

URS Australia Pty Ltd. (2011) Ichthys Gas Fiels Development Project; summary of the long-term water quality program for Darwin Harbour . Repost Prepared by URS Asutralian Pty, Perth, for INPEX Browse, Ltd., Perth., West Autralia.

Wilmott C. J. (1981) On the validations of models, Phys. Geogr., 2, 184-194

APPENDIX A: DELFT3D – A BRIEF MODEL DESCRIPTION

To solve the hydrodynamic problem in adequate spatial and time scales for the final applications (determination of the current field, seal level, and the advection and dispersion of the plume of effluent) and simultaneously maintain reasonable computational costs we opted for the utilization of model Delft3D-FLOW (Deltares, 2016).

The possibility of working with a highly adjustable grid to the coastline contours was another feature that contributed to choose this model. The accommodation of a numerical grid to the shoreline allows an accurate representation of the water body being studied. For the hydrodynamic problem solutions are considered both the mass and momentum conservation equations in spherical coordinates. Also, the hydrostatic and Boussinesq approximations were also used.

In this study non-linear terms of convective acceleration, Coriolis and horizontal turbulent viscosity were considered. Approximation for the use of orthogonal curvilinear coordinates in the numerical solution of the formulation were also considered. These approximations to the numerical grids are used for transformation functions between the physical and the numerical space. Such transformation functions are obtained by solving a set of coupled elliptic partial differential and quasi-linear equations.

The solution of the numerical scheme is initiated by mapping the geometry of the domain into mathematical space from the discretization of the study area in the physical space (definition by the numerical grid). In the mathematical space (regular) the equations of continuity and conservation of momentum are solved. The vertical structure (when requested in the formulation) is determined by explicit procedures with the specification of the terms of horizontal diffusion.

Physical processes

The implementation of the numerical model in the study area was based on a system of three-dimensional shallow water equations. The equations system consists of a set of horizontal motion equations (*momentum*), the equation of continuity and the transport equations for conservative constituents. Such a set of equations is derived from the three-dimensional Navier-Stokes equations for an incompressible fluid. As follows they are described the main considerations and approximations used by the model.

- A sigma vertical coordinate system with five layers (3D) was adopted. The vertical scale (depth) is assumed to be much smaller than the horizontal scale. Thus, due to the reduced aspect ratio, the approximations for the system shallow waters equations become valid, and therefore, the vertical movement of the equation reduces to the hydrostatic equation;
- The Earth curvature effect was not taken into account. Furthermore, the Coriolis parameter was assumed constant;
- A second order formulation was applied in the bottom shear stress;
- Turbulent closures based on the Reynolds tensions;
- Kinetic energy closure proportional to the orders of magnitude of the velocity and the horizontal scale;

- In agreement with the aspect ratio to consideration of shallow waters formulation, the generation of turbulence is based on the vertical gradient of horizontal flow;
- The mass flow in the lateral and in the seabed is null, and
- By not specify the temperature field, the heat exchange with the atmosphere is null. Heat exchange with the seabed is null too.

Sediment transport and morphology

The sediment transport and morphology module supports both bedload and suspended load transport of non-cohesive sediments and suspended load of cohesive sediments. For parameterisation we distinguish “mud” (cohesive suspended load transport), “sand” (non-cohesive bedload and suspended load transport) and “bedload” (non-cohesive bedload only or total load transport) fractions.

In this study a fraction of sediment source from the dredging was implemented in the model and calculated its transport and fates. The delft model uses the hydrodynamics model result to calculate the sediment transport and morphology. The local flow velocities and eddy diffusivities are based on the results of the hydrodynamic computations. Computationally, the three-dimensional transport of sediment is computed in exactly the same way as the transport of any other conservative constituent, such as salinity, heat, and constituents

Reference

Deltares, 2016. Delft3D-FLOW. Simulation of Multi-Dimensional Hydrodynamic and Transport Phenomena, Including Sediments. – User Manual. Delft, The Netherlands.

APPENDIX B: PARTICLE SIZE DISTRIBUTION (PSD)

EA150: Soil Classification based on Particle Size			
Clay (<2 µm)	Silt (2-60 µm)	Sand (0.06-2.00 mm)	Gravel (>2mm)
%	%	%	%
22	13	38	27
17	18	29	36
17	10	39	34
10	22	38	30
15	11	51	23
23	32	22	23
17	11	54	18
21	12	41	26
12	4	47	37
17	9	57	17
14	9	47	30
21	16	41	22
7	11	28	54
12	19	34	35
14	14	55	17
14	15	46	25
12	11	22	55
13	11	30	46
16	18	34	32
15	26	25	34
10	64	13	13
16	13	43	28
11	16	52	21
17	12	43	28
38	12	23	27
8	8	51	33
18	19	37	26
20	20	40	20
32	59	7	2
16	7	46	31
18	12	37	33
18	9	48	25
16	13	58	13
21	20	40	19
1	32	37	30
14	10	31	45
14	13	39	34
23	27	19	31
18	18	44	20
26	28	17	29
18	10	48	24
19	13	46	22
18	14	41	27
13	8	67	12
18	16	41	25